

1 Regional analysis of groundwater droughts using 2 hydrograph classification

3
4 **J.P. Bloomfield¹, B.P. Marchant², S.H. Bricker² and R.B. Morgan³**

5 [1]{British Geological Survey, Wallingford, United Kingdom}

6 [2]{British Geological Survey, Keyworth, United Kingdom}

7 [3]{Environment Agency, Lincoln, United Kingdom}

8 Correspondence to: J. P. Bloomfield (jpb@bgs.ac.uk)

9 10 **Abstract**

11 Groundwater drought is a spatially and temporally variable phenomenon. Here we describe
12 the development of a method to regionally analyse and quantify groundwater drought. The
13 method uses a cluster analysis technique (non-hierarchical *k*-means) to classify standardised
14 groundwater level hydrographs (the Standardised Groundwater level Index, SGI) prior to
15 analysis of their groundwater drought characteristics, and has been tested using 74
16 groundwater level time series from Lincolnshire, UK. Using the test data set, six clusters of
17 hydrographs have been identified. For each cluster a correlation can be established between
18 the mean SGI and a mean Standardised Precipitation Index (SPI), where each cluster is
19 associated with a different SPI accumulation period. Based on a comparison of SPI time
20 series for each cluster and for the study area as a whole, it is inferred that the clusters are
21 independent of the driving meteorology and are primarily a function of catchment and
22 hydrogeological factors. This inference is supported by the observation that the majority of
23 sites in each cluster are associated with one of the principal aquifers in the study region. The
24 groundwater drought characteristics of the three largest clusters, that constitute ~80% of the
25 sites, have been analyzed. There are differences in the distributions of drought duration,
26 magnitude and intensity of groundwater drought events between the three clusters as a
27 function of autocorrelation of the mean SGI time series for each cluster. In addition, there are
28 differences between the clusters in their response to three major multi-annual droughts that
29 occurred during the analysis period. For example, sites in the cluster with the longest SGI
30 autocorrelation experience the greatest magnitude droughts and are the slowest to recover

31 from major droughts, with groundwater drought conditions typically persisting at least six
32 months longer than at sites in the other clusters. Membership of the clusters is shown to be
33 related to unsaturated zone thickness at individual boreholes. This last observation
34 emphasises the importance of catchment and aquifer characteristics as (non-trivial) controls
35 on groundwater drought hydrographs. The method of analysis is flexible and can be adapted
36 to a wide range of hydrogeological settings while enabling a consistent approach to the
37 quantification of regional differences in response of groundwater to meteorological drought.

38

39 **1. Introduction**

40 Groundwater drought is a type of hydrological drought characterised by sustained low
41 groundwater levels, reduced base flow and reduced flows to springs and groundwater-fed
42 rivers and wetlands (Van Lanen and Peters, 2000; Tallaksen and Van Lanen, 2004; Mishra
43 and Singh, 2010; Van Loon, 2015). Like other hydrological aspects of drought, groundwater
44 droughts are not a simple function of meteorological drivers. The impact of droughts on
45 regional groundwater resources can vary in space and time. This is because the response of
46 groundwater systems to meteorological droughts, through changes in groundwater levels and
47 baseflow to groundwater supported rivers, is influenced by spatial variations in intrinsic
48 catchment and aquifer characteristics and processes. These include highly non-linear
49 unsaturated zone processes, recharge, and saturated groundwater storage, flow and discharge
50 over a range of space and time scales (Tallaksen et al, 2009; Bloomfield and Marchant, 2013;
51 Van Lanen et al., 2013; Van Loon and Laaha, 2015).

52 In order to improve the design and operation of groundwater drought monitoring networks,
53 the analysis and interpretation of data from such networks, and, more generally, water
54 resource management at the onset, during and after episodes of groundwater drought, there is
55 a need for a much better understanding of the heterogeneous spatio-temporal response of
56 aquifers to major meteorological droughts (Bloomfield and Marchant, 2013). This includes
57 the need for robust methods to systematically characterise and quantify the heterogeneous
58 response of groundwater to meteorological droughts at a regional scale prior to investigation
59 and attribution of the causes of any heterogeneous response. Despite extensive work on the
60 regional analysis of meteorological and other hydrological droughts, to date there has been no
61 systematic investigation of heterogeneities in groundwater droughts at the regional scale. This
62 paper describes the application of one such suite of methods to regionally analyse

63 groundwater level hydrographs and to assess variations in the spatial response of groundwater
64 to meteorological droughts using a case study from the UK.

65 **1.1 Controls on spatial heterogeneity in groundwater drought**

66 A few previous studies have presented evidence for the spatially heterogeneous response of
67 groundwater to meteorological droughts. To help develop an optimal monitoring network for
68 groundwater resources under drought conditions, Chang and Teoh (1995) described the
69 heterogeneous response of groundwater levels at 13 observation boreholes to meteorological
70 droughts across a basin in Ohio, USA, although they did not investigate the hydrogeological
71 causes of the heterogeneity. Van Lanen (2005) and Van Lanen and Tallaksen (2007)
72 observed that drought characteristics derived from groundwater levels have ‘spatial effects’,
73 and noted that these spatial effects on groundwater drought are an important consideration
74 when monitoring droughts using groundwater levels. Van Lanen and Tallaksen (2007)
75 compared modelled groundwater recharge and discharge for a humid continental climate
76 (Missouri, USA) and a tropical savannah climate (Guinea) for quick- and slow-responding
77 catchments and showed that both climatology and the responsiveness of the catchment as
78 defined by the aquifer characteristics have an influence on drought generation. Peters et al.
79 (2006) investigated the propagation and spatial distribution of aspects of modelled
80 groundwater drought, including recharge, groundwater level and groundwater discharge in
81 the Pang catchment in the UK. They found that short droughts in groundwater levels were
82 most severe near streams and were attenuated with distance from the streams; longer periods
83 of below average recharge had more effect on suppressing groundwater levels on interfluvies
84 near groundwater divides, and that droughts in groundwater discharge are more attenuated
85 upstream and less so downstream in the catchment. Tallaksen et al. (2009) also modelled the
86 spatio-temporal response of the Pang catchment to drought events and found large differences
87 between the spatio-temporal response of groundwater recharge, level and discharge and the
88 driving meteorological droughts, where droughts in groundwater recharge and levels were
89 found to cover relatively small areas, but last longer, than the meteorological droughts.

90 Mendicino et al. (2008) developed a groundwater resource index for drought monitoring and
91 forecasting based on a simple distributed runoff/water balance model, and evaluated the use
92 of the index in three catchments in southern Italy. They found that the groundwater resource
93 index was highly spatially variable and related it to variations in hydraulic conductivity
94 across the catchments. Using a newly developed groundwater drought index, the

95 Standardised Groundwater level Index (SGI), Bloomfield & Marchant (2013) also
96 investigated hydrogeological controls on groundwater drought. Based on 14 observation
97 boreholes in different catchments across England, UK, they showed that groundwater drought
98 duration depended on the autocorrelation structure of SGI time series. This was in turn
99 inferred to be both a function of spatially varying recharge processes and saturated flow
100 processes within the local aquifer systems.

101 **1.2 Regional analysis of groundwater drought**

102 There has been significant work on the regional analysis of meteorological and other
103 hydrological droughts. Cluster Analysis (CA), Principal Component Analysis (PCA) or some
104 combination of both techniques have been used extensively by meteorologists and
105 hydrologists to investigate the spatio-temporal distribution of hydrological variables,
106 including drought indices (e.g. Klugman ,1978; Karl and Koscieny, 1982; Eder et al., 1987;
107 Stahl and Demuth, 1999; 2001, Lana et al., 2001; Bonaccorso et al., 2003; Vicente-Serrano,
108 2006; Vicente-Serrano and Cuadrat-Prats, 2007; Raziell et al., 2008; Santos et al., 2010; Fleig
109 et al., 2011; Hannaford et al., 2011; Lorenzo-Lacruz et al., 2013).

110 Although not previously applied to groundwater drought, CA and/or PCA techniques have
111 been used to classify groundwater level hydrographs for a range of purposes. Winter et al.
112 (2000) classified groundwater hydrographs from three small lake-dominated catchments to
113 investigate groundwater recharge and differences in the hydrographs as a function of the
114 geology of the catchments. Similarly, Moon et al. (2004) applied PCA to 66 groundwater
115 level hydrographs from South Korea to characterise the spatial variability in groundwater
116 recharge. Upton and Jackson (2011) used CA and PCA (following a methodology developed
117 by Hannah et al., 2000) with 52 groundwater level hydrographs from the Pang and Lambourn
118 catchments in the UK to produce regional or ‘master’ hydrographs for modelling the spatial
119 distribution of groundwater flooding.

120 Here we present the first systematic regional analysis of groundwater droughts using a case
121 study from Lincolnshire, UK. The case study consists of 74 groundwater hydrographs from
122 an area of approximately 8,000 km² that includes three regionally important aquifers, the
123 Lincolnshire Limestone, the Chalk and the Spilsby Sandstone aquifers, each with contrasting
124 aquifer characteristics (section 2). The groundwater hydrographs have been normalised using
125 the Standardised Groundwater level Index (SGI) technique of Bloomfield & Marchant (2013)
126 and groups or clusters of similar groundwater hydrographs have been identified using CA,

127 where hydrogeologically meaningful clusters are identified by explicitly searching for groups
128 of hydrographs that can be explained by *a posteriori* knowledge of the groundwater system
129 (section 4.2). The drought characteristics of the clusters have been quantified in terms of
130 drought event duration, magnitude and intensity and the impact of the three major, multi-
131 annual droughts on the SGI time series has been investigated (section 4.4). Controls on the
132 groundwater drought response in each of the clusters have been explored and the results
133 briefly discussed in terms of the implications for monitoring and managing groundwater
134 droughts (section 5).

135

136 **2. The case study**

137 The case study area of Lincolnshire is situated in the east of England, UK. It is bounded by
138 the North Sea to the east, the Wash estuary to the south and the Humber Estuary to the north
139 (Fig. 1). The area is predominantly rural with highly productive agricultural and horticultural
140 land, fens and estuarine wetlands. Lincoln, Boston and Scunthorpe are the principal small
141 conurbations in the study area. The land is generally flat and low-lying, typically less than 30
142 m above sea level (m asl), apart from the Chalk of the Lincolnshire Wolds and the
143 Lincolnshire Limestone outcrop which form northwest-southeast trending escarpments that
144 reach elevations of approximately 150 m asl and 70 m asl respectively.

145 **2.1 Hydrometeorology and drought history**

146 As a first-order approximation, it is assumed that the broad meteorological drought history of
147 the study area is spatially homogeneous. This assumption means that any relative differences
148 in drought histories between sites or clusters need to be explained in terms of catchment or
149 hydrogeological factors, rather than differences in the drought climatology. This assumption
150 is tested as part of the analysis of correlations between precipitation and regional
151 groundwater levels (see section 4.2). It is also supported by the observations that the whole
152 study area is governed by the same broad climatic patterns, i.e. rain-bearing low pressure
153 systems from the Atlantic and high pressure systems leading to a lack of rainfall, with only
154 small variation in annual precipitation across the region (Marsh and Hannaford, 2008). The
155 assumption is also consistent with the previously documented spatial coherence of major
156 hydrological (surface water) droughts in the UK (Hannaford et al., 2011; Fleig et al., 2011;
157 Folland et al., 2015) where the current study area falls within a homogeneous drought region
158 (“region 4” of Hannaford et al., 2011, “region GB4” of Fleig et al., 2012; Kingston et al.,

159 2013, and the “English Lowlands” of Folland et al., 2015) although it is noted that the effects
160 of landscape processes can cause heterogeneous meteorological signals to become attenuated
161 (Van Loon, 2015).

162 Mean annual rainfall varies across the study area from about 600 to 700 mm (Marsh and
163 Hannaford, 2008). The groundwater hydrographs used in the study have been analysed from
164 1983 to 2012. During this period, three multi-annual episodes of drought have previously
165 been documented by Marsh et al. (2007; 2013), Kendon (2013), Parry and Marsh (2013) and
166 Folland et al. (2015) as follows: 1988 to 1992, 1995 to 1997 and 2010 to 2012. All are known
167 to have been major drought events causing reduced surface flows and suppressed
168 groundwater levels throughout large areas of central, eastern and southern UK as well as over
169 parts of North West Europe (Lloyd-Hughes and Saunders, 2002; Lloyd-Hughes et al., 2010;
170 Hannaford et al., 2011; Fleig et al., 2012 and Kingston et al., 2013).

171 **2.2 Geology and hydrogeology**

172 The study area consists of a sequence of Jurassic and Cretaceous aquifers separated by low
173 permeability clay and shale units. The whole sequence generally dips gently eastwards and
174 where each of the aquifer units passes under an overlying low permeability formation they
175 typically become confined. The whole sequence is unconformably overlain by Quaternary
176 superficial deposits. Figure 1 shows the distribution of the three main aquifers in the region:
177 the Jurassic Lincolnshire Limestone; the Lower Cretaceous/Upper Jurassic Spilsby
178 Sandstone, and the Upper Cretaceous Chalk, and includes a schematic cross-section of the
179 hydrostratigraphy of the study area. These aquifers are hydrogeologically distinct from each
180 other, and two of them, the Lincolnshire Limestone and the Chalk have previously
181 documented spatially variability. Below we summarise these features as they inform the
182 heuristic rules used in section 4.2 to guide the selection of clusters as part of the CA.

183 The Lincolnshire Limestone Formation is an oolitic limestone with fine-grained, micritic and
184 peloidal units (Allen et al., 1997), and is up to 40 m thick at outcrop in the west. It dips and
185 thins to the east where it becomes confined and eventually pinches out down-dip. Maximum
186 unsaturated zone thickness is up to about 45m towards the southwest of the outcrop.
187 Groundwater movement is almost entirely by fracture flow along well-developed bedding
188 plane fractures and joints. Abstraction takes place mainly from the region immediately to the
189 east of the outcrop. It has highly variable transmissivities and storage coefficients typical of a
190 fractured limestone. Allen et al. (1997) have reported a wide range of transmissivity values

191 for the Lincolnshire Limestone with an interquartile range of 260 to 2260 m² d⁻¹ and a
192 geometric mean of 660 m² d⁻¹, with slightly higher transmissivities being reported from the
193 south of the region, and a very wide range of storage coefficients from 2x10⁻⁷ to 0.58.

194 The Spilsby Sandstone aquifer is up to about 30 m thick consisting of a variably, but often
195 poorly cemented pebbly quartz sandstone with alternating thin clays and marls (Whitehead
196 and Lawrence, 2006). It outcrops along the foot of the Wolds escarpment (Fig. 1) where it is
197 associated with springs and maximum unsaturated zone thickness is about 30m. It dips to the
198 east and away from outcrop and it is generally confined by clays above and below (Fig. 1).
199 Jones et al., (2000) reported transmissivity values in the range 130 to 170 m² d⁻¹, and a
200 geometric mean of 140 m² d⁻¹ with storage coefficients ranging from 1x10⁻⁴ to 1x10⁻³ and
201 with a geometric mean of 4x10⁻⁴.

202 The Chalk is a microporous fractured limestone (Bloomfield et al, 1995). Storage and
203 transmissivity are controlled by local sub-karstic development of the fracture network
204 (Bloomfield, 1996; Maurice et al., 2006). The Chalk Group reaches a thickness of over
205 250 m. Groundwater flows from the recharge areas in the west eastward down dip towards
206 and into the confined Chalk to the east. The Chalk bedrock surface was significantly altered
207 during the Ipswichian interglacial of the Quaternary. As a result of glacial activity a cliff line
208 and wavecut platform were eroded into the Chalk (Fig. 1). The Chalk to the east of the
209 palaeo-cliff line is now buried beneath a covering of till, sand and gravel superficial deposits
210 (Whitehead and Lawrence, 2006). Maximum unsaturated zone thickness occurs towards the
211 northwest of the Chalk outcrop and is about 60m contrasting with the relatively thin
212 unsaturated zone to the east of the palaeo-cliff line. Allen et al. (1997) and Whitehead and
213 Lawrence (2006) have reported that transmissivity values differ between the northern and
214 southern Chalk in Lincolnshire. In the northern part of the region transmissivity has an
215 interquartile range of 1020 m² d⁻¹ to 6070 m² d⁻¹ with a geometric mean of 2350 m² d⁻¹,
216 whereas in the southern area, in the region of the eroded Chalk, transmissivity is slightly
217 reduced and has an interquartile range of 850 m² d⁻¹ to 3010 m² d⁻¹ with a geometric mean of
218 1380 m² d⁻¹. Similarly, Allen et al. (1997) report storage coefficients with an interquartile
219 range of 3.5x10⁻⁵ to 1.5x10⁻³ and with a geometric mean of 2x10⁻⁴ for the northern Chalk and
220 6.1x10⁻⁵ to 2.7x10⁻³ and with a geometric mean of 1.5x10⁻³ for the southern Chalk.

221 The Quaternary superficial deposits in the study area comprise: glaciofluvial sand and gravels
222 and tills; peat; tidal flat deposits; river terrace sands and gravels, and overlying alluvium.

223 The Lincolnshire Limestone Formation and the western part of the Chalk outcrop are largely
224 absent of superficial cover.

225

226 **3. Data and Methods**

227 **3.1 Data**

228 Groundwater level data for the 74 observation boreholes (Fig. 1) has been provided by the
229 Environment Agency from their groundwater level monitoring network database
230 (Environment Agency, 2014). Prior to the study none of the sites were believed to be
231 significantly impacted by abstraction although all three regional aquifers are used for public
232 water supply, abstractions for agricultural irrigation and industrial use (Allen et al., 1997;
233 Whitehead and Lawrence, 2006). Where observation boreholes penetrate both the Chalk and
234 underlying Spilsby Sandstone aquifer, the boreholes are completed with screens so that they
235 monitor water levels in only one of the two aquifers. Groundwater levels have been recorded
236 over a range of frequencies, but typically at weekly to monthly time steps. Based on the raw
237 groundwater level data, mean monthly groundwater levels have been estimated. If no
238 observations were available for a given month then a linear interpolation was used to estimate
239 the monthly groundwater levels following the method described by Bloomfield and Marchant
240 (2013).

241 Precipitation data has been taken from the Centre for Ecology and Hydrology's Continuous
242 Estimation of River Flows (CERF) 1km gridded precipitation dataset (Keller et al., 2005;
243 Dore et al., 2012; Bloomfield and Marchant, 2013). CERF daily gridded precipitation data is
244 generated from rain gauge data held in the UK Met Office national precipitation monitoring
245 network. A triangular planes methodology is used to produce a daily 1km² grid based on a
246 weighted average (inverse distance) of the three nearest rain gauges. Daily rainfall is then
247 summed to give total monthly gridded rainfall. The precipitation data that is used with each
248 groundwater level observation site is the monthly total for the CERF 1km² grid square that
249 contains the given groundwater observation borehole.

250 **3.2 Methods**

251 **3.2.1 Hydrograph normalisation using the SGI method**

252 The groundwater level hydrographs have been normalised to the Standardised Groundwater
253 level Index (SGI) of Bloomfield and Marchant (2013). This is a non-parametric

254 normalization of data that assigns a value to the monthly groundwater levels based on their
255 rank within groundwater levels for a given month from a given hydrograph. The normal
256 scores transform is undertaken by applying the inverse normal cumulative distribution
257 function to n equally spaced p_i values ranging from $1/(2n)$ to $1 - 1/(2n)$. The values that result
258 are the SGI values. They are then re-ordered such that the largest SGI value is assigned to the
259 i for which p_i is largest, the second largest SGI value is assigned to the i for which p_i is
260 second largest and so on. In summary, for each of the 74 study sites, normalized indices are
261 estimated from the groundwater level data for each calendar month using the normal scores
262 transform. These normalized indices are then merged to form a continuous SGI. Precipitation
263 records for each site have also been normalised. At each site a version of the Standardised
264 Precipitation Index (SPI) after McKee et al. (1993) has been estimated for precipitation
265 accumulation periods of 1, 2, ..., 36 months. For consistency between groundwater and
266 precipitation indices, SPIs are estimated using the normal scores transform applied to
267 accumulated precipitation data for each calendar month.

268 **3.2.2 Cluster analysis**

269 Cluster Analysis (CA) attempts to identify clusters of similar individuals amongst a
270 multivariate dataset. In the context of this paper CA is used to form clusters of groundwater
271 level hydrographs which exhibit similar fluctuations in their SGI time series. A wide range of
272 CA algorithms exist. They are most coarsely distinguished according to whether or not they
273 assume that the resultant clusters are hierarchical. Given the wide variety of algorithms it is
274 difficult to decide upon the best approach to cluster a particular dataset. Webster and Oliver
275 (1990) stress that this decision is rather subjective, although previous studies that have used
276 CA to cluster hydrographs have typically justified their choice of algorithm by claiming that
277 some produce more physically interpretable groupings. For example, Hannah et al. (2000)
278 used the agglomerative hierarchical average linkage algorithm as they thought it was more
279 interpretable than alternatives such as the centroid and Ward's clustering procedures. Webster
280 and Oliver (1990) recommend that multiple clustering algorithms should be applied and
281 expert knowledge of the system being investigated used to decide which set of clusters is
282 most relevant. In this paper we adapt this approach by applying one hierarchical and one non-
283 hierarchical method.

284 Hierarchical classifiers require a measure of the similarity (or dissimilarity) between each
285 pair of individuals. Common examples include the Euclidean distance or the correlation
286 between the measurements of the individuals. The pairwise similarities between s individuals

287 are expressed in a $s \times s$ matrix **B**. A mathematical criterion is then used to allocate the
288 individuals to different clusters in a manner that maximizes the similarity between the
289 individuals within the groups whilst minimizing the similarity between individuals in
290 different clusters. For our hierarchical clusters we measure the similarity between
291 groundwater level hydrographs by the correlation matrix of their SGI time series and then
292 apply the agglomerative hierarchical complete-linkage strategy (Webster and Oliver, 1990) to
293 merge the boreholes into clusters.

294 We also apply the commonly used non-hierarchical k -means clustering algorithm. It is widely
295 used in spatial analysis studies, for example, Santos et al. (2010), Raziei et al. (2012) and
296 Sadri et al. (2014) have all used the k -means clustering algorithm to investigate the regional
297 characteristics of droughts. The approach partitions the individuals into a specified number of
298 clusters. A numerical optimization routine is used to select the partitioning which maximizes
299 the similarity between each individual and the centroid of the cluster in which it is contained.
300 Again there is flexibility in the choice of similarity measure and the manner in which the
301 centroid of a cluster is calculated. We use the squared Euclidean distance between the vectors
302 of time series observations from each site to assess similarity and define the centroid of a
303 cluster as the multi-dimensional mean of the time series within the cluster.

304 Clustering methods do not produce a unique partitioning of a given data set on their own, and
305 for both the hierarchical and non-hierarchical approaches there remains the issue of deciding
306 upon the optimal number of clusters. This can be achieved by asking an expert on the system
307 in question to compare the attributes of clusterings consisting of a different number of
308 groups. Here we use a rule-based approach to help identify the number of clusters based on
309 knowledge of the general hydrogeology of the study area. Bloomfield and Marchant (2013)
310 have previously shown that groundwater drought characteristics are a function of unsaturated
311 zone thickness in fractured aquifers such as the Lincolnshire Limestone and Chalk aquifers,
312 and that when a broader range of aquifer types are considered groundwater drought
313 characteristics are also a function of the hydraulic diffusivity of aquifers. Here we use these
314 observations and knowledge of the spatial variation in these features across the three aquifers
315 in the study area (section 2.2) to design rules to aid in the selection of clusters. The rules
316 adopted for the current study are to identify the smallest number of clusters that: i.) broadly
317 resolve the spatial distribution of the three aquifers across the study region, ii.) given the
318 previously documented N-S variation in aquifer properties and unsaturated zone thickness
319 across the Lincolnshire Limestone aquifer (Allen et al., 1997), that distinguish more than one

320 region of the Lincolnshire Limestone, and iii.) given variations in aquifer properties and
 321 unsaturated zone thickness across the Chalk aquifer both N-S and across the buried cliff line
 322 (Allen et al., 1997), that distinguish more than one region of the Chalk. Note that this set of
 323 rules is specific to the current study, however, for any given study area the target number of
 324 classes and hence the rules used can be adapted to reflect the regional hydrogeology and in
 325 particular any knowledge of heterogeneity in the aquifer systems under investigation.
 326 However, mathematical criteria can also be used as a guide to clustering. We also calculate
 327 the RMSSD, the square root of sum of the squared Euclidean distance between each
 328 individual and the centroid of the group to which it is allocated. In combination with expert
 329 judgement related to the system under consideration, it is common practice to inform the
 330 choice of the number of clusters using plots of RMSSD versus cluster number. Since RMSSD
 331 decreases non-linearly as the number of clusters increases, a cluster number is selected
 332 associated with a decrease in the rate of RMSSD decline.

333 **3.2.4 Autocorrelation structure of the SGI time series**

334 Bloomfield and Marchant (2013) demonstrated the importance of the autocorrelation
 335 structure of SGI time series for groundwater drought studies by establishing a relationship
 336 between the range of significant autocorrelation in the SGI series, m_{\max} , and corresponding
 337 SPI. They showed that m_{\max} scales linearly with q_{\max} , where q_{\max} is the SPI accumulation
 338 period which leads to the strongest correlation between SGI and SPI. Both m_{\max} and q_{\max} are
 339 also used here to characterise and quantify groundwater droughts within each of the clusters
 340 of groundwater hydrographs and have been estimated as follows.

341 If the mean SGI for a borehole is denoted by $\overline{\text{SGI}}$ then the k th sample autocovariance
 342 coefficient is defined to be

$$343 \quad g_k = \frac{1}{n} \sum_{i=k+1}^n \{\text{SGI}(i) - \overline{\text{SGI}}\} \{\text{SGI}(i - k) - \overline{\text{SGI}}\} \quad (1)$$

344 and the k th sample autocorrelation coefficient is

$$345 \quad r_k = \frac{g_k}{g_0} \quad (2)$$

346 where g_0 reduces to the population variance function (see Eqn. 1 when $k = 0$). The
 347 correlogram is a plot of r_k against k . If there is no correlation between the $\text{SGI}(i)$ observed k
 348 months apart and if the SGI values are normally distributed then r_k is approximately normally
 349 distributed with mean zero and variance $1/n$. Therefore values of r_k with magnitude greater

350 than $2/\sqrt{n}$ indicate significant correlation at approximately the 5 % level. We define the
351 range of significant temporal correlation of a SGI time series to be the largest m , m_{\max} , for
352 which $r_k > 2/\sqrt{n}$ for all $k \leq m$. Since all of our groundwater records are of $n = 355$ months
353 the threshold on r_k is equal to 0.11. To estimate q_{\max} , Pearson correlation coefficients are
354 calculated between SGI and SPI with accumulation periods of $q = 1, 2, \dots, 36$ months and
355 the accumulation period associated with the maximum correlation gives q_{\max} .

356

357 **4. Results**

358 **4.1 Identification of regional droughts from average SPI and SGI time series**

359 Before undertaking the regional drought analysis, the correlation between mean SPI and SGI
360 for the entire region, based on all 74 sites, has been investigated and the large-scale drought
361 history of the study area has been defined.

362 Figure 2a is a heatmap showing the correlation coefficient between SPI for precipitation
363 accumulation periods $q = 1$ to 36 months and SGI for lags between SPI and SGI of 0 to 5
364 months based on average values of SPI and SGI for all 74 sites. Dark blue denotes zero
365 correlation and dark red a perfect correlation. Figure 2a shows that there is a good
366 correlation between SPI and SGI. The strongest correlation (0.84, denoted by the closed black
367 circle in Fig. 2a) is for a precipitation accumulation period (q_{\max}) of 12 months (SPI_{12}) with
368 no lag between the SGI and SPI time series. This is consistent with the observations of
369 Bloomfield and Marchant (2013) who previously reported q_{\max} for a variety of groundwater
370 hydrographs from the UK with an average of 13 months and Folland et al. (2015) who
371 reported a q_{\max} of 12 months for aggregated time series representing the English Lowlands.
372 Figures 2b and 2c, the average SPI_{12} and SGI time series respectively, have similar features.
373 For example, episodes of high groundwater levels in 1983, 1994, 2002, and 2008 correspond
374 with high values of SPI_{12} . Three episodes of regionally significant groundwater drought
375 associated with prolonged low groundwater levels from October 1988 to November 1993,
376 May 1995 to February 1998, and from August 2010 to August 2012 correspond closely with
377 episodes of meteorological drought in the SPI_{12} time series and are consistent with those
378 identified by previous studies (Lloyd-Hughes and Saunders, 2002; Marsh et al., 2007; 2013;
379 Kendon, 2013; Hannaford et al., 2011; Parry and Marsh, 2013; Folland et al., 2015). It is
380 inferred from these observations that the large-scale drought history of the study area is
381 represented well by the average SPI_{12} and SGI time series.

382 4.2 Regional analysis of the SGI hydrographs

383 CA has been used to analyse the heterogeneous response of groundwater to droughts across
384 the study region. Clustering has been undertaken using both an agglomerative hierarchical
385 complete-linkage algorithm and a non-hierarchical k -means clustering algorithm and the
386 resulting clusters searched for those that are hydrogeologically meaningful and that can be
387 explained by known features of the catchment and groundwater systems. Figure 3a is a
388 dendrogram that fully illustrates the level of similarity between individuals within the clusters
389 formed by the hierarchical clustering. The number of clusters is controlled through the
390 threshold on the distance between groups. For example, a threshold of 0.62 leads to the six
391 clusters shown in Fig. 3b. Figure 3c is an equivalent map showing the distribution of sites by
392 clusters formed by k -means clustering for $k = 6$.

393 Figures 3b and 3c shows that the spatial distribution of sites as a function of the clusters
394 formed by the hierarchical and non-hierarchical approaches are broadly similar, so the choice
395 of clustering algorithm is based on a plot of RMSSD against number of clusters. Figure 4
396 shows that the RMSSD for the k -means clustering is systematically lower than that for the
397 hierarchical clustering algorithm where there are three clusters or more, so we have chosen to
398 use the non-hierarchical k -means clustering approach. Note also that both clustering
399 algorithms are better than a clustering scheme based solely on the three classes of aquifer
400 (e.g. Lincolnshire Limestone, Chalk and Spilsby Sandstone). However, an optimal number of
401 k -mean clusters is not clearly evident in Fig. 4. After careful inspection of the clusters formed
402 by a range of k -means clustering classes and a consideration of the study specific clustering
403 rules described in section 3.2.2, $k = 6$ was selected. Based on k -means clustering where
404 $k = 6$, Fig. 3c shows the distribution of sites between the six clusters (cluster 1 to cluster 6,
405 or CL1, ... CL6).

406 It can be seen from Fig. 3c that the resulting k -means clusters have a degree of spatial
407 coherency. We have previously assumed that such spatial correlations in the SGI time series
408 are primarily a function of catchment and hydrogeological factors and not a consequence of
409 heterogeneity in the driving meteorology. Here we test if this is the case, prior to further
410 exploration of the features of each cluster, by investigating if precipitation associated with
411 each cluster is substantially different from regional average precipitation. To do this, we first
412 need to identify a representative accumulation period, q_{\max} , for precipitation for each cluster.

413 Figure 5 is a set of heatmaps, similar to Fig. 2a, showing the correlation between SPI for
414 precipitation accumulation periods, q , 1 to 36 months, and SGI for lags between SPI and SGI
415 time series of 0 to 5 months for each of the six clusters. Dark blue denotes zero correlation
416 and dark red a perfect correlation with the strongest correlation for each cluster marked by
417 the closed black circle. Table 1 gives q_{\max} for each cluster and also gives the maximum
418 associated correlation coefficient. In all cases, except CL2, the maximum correlation
419 between SPI and SGI is found where there is no lag between the two time series. For CL2 it
420 is found at a lag of one month. The highest correlations are for CL2, CL4 and CL1 at 0.86,
421 0.82 and 0.74 respectively. The correlations for CL3 and CL5 are moderate (0.36 and 0.53)
422 and for CL6 there is effectively no correlation (0.09). This is consistent with the observations
423 made in section 4.3 below that linear trends in CL3 and CL5 appear to affect the SGI time
424 series and that the SGI hydrograph for CL6 appears to be anomalous, departing from the
425 mean regional SGI and SPI signals. Values of q_{\max} for CL1 to CL5 from Fig. 5 are 4, 16, 15,
426 9, and 17 months respectively. Based on these, Fig. 6 shows SPI time series for each cluster,
427 where black lines are the mean SPI for the cluster and the red lines are average SPI across the
428 study area based on the same cluster-specific q_{\max} . Since Fig. 6 illustrates that the two SPI
429 time series for each cluster are similar, we infer that heterogeneity in the driving meteorology
430 across the study region, or at least between the clusters as defined here, does not play an
431 important role in the clustering process and that membership of clusters is dominated by
432 catchment or hydrogeological factors.

433 **4.3 Characteristic features of the SGI hydrograph clusters**

434 Figure 7 shows the mean SGI time series for each cluster. Two main qualitative observations
435 can be made regarding the SGI hydrographs. Five of the six clusters have a similar overall
436 form to the mean SGI hydrograph for the region (Fig. 2c) showing common patterns of low
437 (and high) groundwater level stand. Whereas, CL6 appears to be an exception with a different
438 overall form to the SGI hydrograph – it also exhibits an anomalous step change in SGI from
439 drought to high groundwater level stand over an eight month period from May 1990 to
440 December 1990. Secondly, two of the clusters, CL3 and CL5, appear to show declining linear
441 trends in SGI making direct comparison of drought histories between these and other clusters
442 problematic.

443 Bloomfield & Marchant (2013) have previously shown that m_{\max} , a measure of the significant
444 autocorrelation length of SGI time series, relates to features of groundwater drought. A

445 similar analysis of autocorrelation structure of SGI time series for each cluster is presented
446 here. Figure 8 shows autocorrelation plots for SGI hydrographs for each of the six clusters. In
447 each figure the pale grey lines are autocorrelation plots for individual sites and the solid black
448 line is the autocorrelation plot for the mean SGI time series for the cluster with the horizontal
449 dashed line indicating the significant level of autocorrelation based on the record length.
450 Based on these plots, values of m_{\max} for the mean SGI time series for each cluster are given in
451 Table 1. Values of m_{\max} for CL3, CL5 and CL6 are anomalously large, consistent with the
452 anomalous features of these SGI hydrographs described above. For the remaining clusters,
453 Figure 8 and Table 1 show that CL1 has the shortest autocorrelation of 15 months. In
454 comparison, CL2 has an autocorrelation of 23 months and CL4 is intermediate at 18 months.

455 These contrasting characteristics between the clusters can be seen clearly in Fig. 9a which
456 illustrates SGI time series for all sites within each cluster, grouped in their respective clusters,
457 and presented in the form of a heatmap where low values of SGI (associated with drought
458 conditions) are in shades of green to red (increasing drought intensity) and episodes of high
459 groundwater level stand are in shades of green to blue (increasing high groundwater levels).
460 The three major episodes of drought can be seen clearly in the heatmaps for CL1, CL2 and
461 CL4, but are obscured by the trends in CL3 and CL5 and absent in CL6. The degree of
462 coherency of individual SGI time series within each cluster also appears to be consistent with
463 differences in autocorrelation between the clusters. Figure 9b is a heatmap of the cross-
464 correlation coefficients for all the individual SGI time series ordered as a function of the six
465 clusters, where dark red denotes high correlations and dark blue denotes low correlations.
466 Sites within CL1 and CL4, clusters with moderate or short autocorrelation, show relatively
467 low levels of internal coherency compared with sites in CL2 with relatively long
468 autocorrelation that are highly correlated.

469 Based on the above, the following is a summary of the features of each cluster:

- 470 • CL1 is dominated by sites from the northern parts of the Lincolnshire Limestone. The
471 mean SGI time series of CL1 has a relatively short autocorrelation (m_{\max} of 15 months)
472 and within the cluster SGI hydrographs are relatively variable.
- 473 • CL2 is dominated by sites from the northern part of the Chalk. The cluster has the longest
474 mean SGI autocorrelation (m_{\max} of 23 months) and hydrographs within CL2 are highly
475 correlated indicating a high degree of coherency in groundwater levels across the northern
476 part of the Chalk in the study area.

- 477 • CL3 is a relatively small cluster of six sites, four of which are from the confined Spilsby
478 Sandstone and two from the Lincolnshire Limestone. The main feature of the cluster is a
479 trend in decreasing SGI across the observational record. This trend is consistent with a
480 previous water balance assessment for the Spilsby Sandstone (Whitehead and Lawrence,
481 2006) where annual groundwater deficits have been reported. The sites in this cluster are
482 inferred to be possibly variably impacted by long-term abstraction. Given this inference
483 and the small size of the cluster of sites, CL3 is not included in the subsequent analysis of
484 groundwater droughts.
- 485 • CL4 is dominated by sites from the southern Lincolnshire Limestone and also includes
486 five unconfined sites on the southern Chalk and one site located in the northern
487 Lincolnshire Limestone. It has a moderate autocorrelation, m_{\max} of 18 months. Individual
488 SGI hydrographs within the cluster show a moderate degree of coherency.
- 489 • CL5 is a small cluster of five sites all from the southeastern Chalk to the east of the
490 palaeo-wave cut platform and are the five sites closest to the coast. It has a moderately
491 long autocorrelation, m_{\max} of 28 months that may be affected by an apparent weak trend
492 in declining SGI - there is only a weak correlation between SPI and SGI. Given the small
493 size of the cluster and the apparent trend in mean SGI, CL5 is not included in the
494 subsequent analysis of groundwater droughts.
- 495 • CL6 consists of three SGI hydrographs from the confined Spilsby Sandstone aquifer. The
496 hydrographs are characterised by an anomalous step change in SGI from drought to high
497 groundwater level stand over an eight month period from May 1990 to December 1990.
498 The mean SGI hydrograph shows no correlation with the other five clusters and there is
499 no correlation between SPI and SGI within the cluster. All three sites are within a radius
500 of about 3 km of a public water supply borehole and it is inferred that groundwater levels
501 may be influenced by abstraction. So, as with CL3 and CL5, this very small cluster is not
502 included in the subsequent analysis of groundwater droughts.

503 **4.4 Analysis of droughts using the hydrographs from CL1, 2 and 4**

504 Clusters CL1, CL2 and CL4 consist of 61 of the 74 hydrographs analysed. Here the
505 characteristics of groundwater droughts in these clusters are quantified and the response of
506 the clusters to three major drought episodes is investigated.

507 The duration, magnitude and mean intensity of groundwater drought events have been
508 investigated based on an analysis of the SGI hydrographs where, following the convention of

509 McKee et al. (1993), negative values of SGI denote drought conditions (note, however, that
510 the current convention of the World Meteorological Organisation for SPI refers to drought
511 conditions where SPI is continuously negative and reaches an intensity of -1.0 or less and
512 that negative values between 0 and -1 are classified as near normal and simply indicate less
513 than a median precipitation, World Meteorological Organisation, 2012). Groundwater
514 drought duration, D , is taken to be the total number of consecutive months where SGI is
515 negative. Groundwater drought magnitude, M , is taken to be the total cumulative value of
516 monthly SGI for a given drought event, and mean drought intensity, I , is given by M/D .
517 Summary drought statistics for CL1, CL2 and CL4 are given in Table 2.

518 Table 2 shows that there are differences in the character of the groundwater drought events in
519 the SGI hydrographs for clusters CL1, CL2 and CL3. For example, CL1 has more than twice
520 the number of drought episodes (39 episodes) than CL2 (15 episodes) and the average and
521 maximum duration of droughts in CL1 (4.6 and 27 months respectively) are less than half
522 those of CL2 (11.3 and 61 months). The mean drought event magnitude in CL1 (-2.9) is less
523 than half that in CL2 (-7.9) and the mean drought event intensity in CL1 (-0.43) is almost
524 twice that of CL2 (-0.28). In all cases, the drought event statistics for CL4 fall between those
525 for CL1 and CL2. In summary, CL1 exhibits shorter, but generally more intense drought
526 episodes compared with CL2, with CL4 drought events being of intermediate character.
527 These relative drought phenomena are a consequence of the degree of autocorrelation in the
528 respective SGI time series, where CL1 has a relatively short autocorrelation compared with
529 relatively long autocorrelation for CL2. This observation is consistent with previous site
530 specific and modelling studies that noted a similar relationship between the 'flashiness' or
531 responsiveness of the groundwater system to meteorological divers and the number of
532 droughts, where quickly responding groundwater systems typically experience more droughts
533 than more slowly responding catchments (Peters et al. 2003; Van Loon and Van Lanen, 2012;
534 Van Lanen et al. 2013).

535 There is a strong relationship between drought duration and magnitude for all three clusters,
536 Fig. 10, where longer episodes of groundwater drought are associated with droughts of
537 greater magnitude. However, there is no such regular or simple relationship between drought
538 duration and intensity. Maximum drought intensity is similar for all three clusters, for CL1,
539 CL2 and CL4 it is -1.10, -1.05 and -1.13 respectively (Table 2 and Fig. 11), and is associated
540 with two of the major drought events, i.e. with the latter part of the 1988 to 1993 drought for
541 CL2, and the 2010 to 2012 drought for CL1 and CL4. Figure 11 shows frequency plots of D ,

542 M and I for clusters CL1, CL2 and CL4. A cumulative frequency plot of drought duration
543 (Fig. 11) shows that the distribution in all three clusters is highly positively skewed with
544 many short drought events and relatively few long drought events. As previously noted, the
545 longest duration droughts are associated with CL2, the cluster with the longest
546 autocorrelation in the SGI time series. These observations are consistent with those of Hisdal
547 and Tallaksen (2003), Tallaksen et. al. (2009) and Fleig et al. (2011) who have also described
548 strongly skewed distributions of hydrological drought durations.

549 Three major, multi-annual droughts have already been described from the regional (Fig. 2)
550 and the cluster-specific (Figs. 7 and 9a) SGI time series. Table 3 summarises differences in
551 the relationships between the driving meteorology and the drought characteristics of each
552 cluster for the three major droughts. Each of the major drought episodes have been quantified
553 using drought characteristics as applied to SPI_{12} and SGI for each of the clusters.

554 The 1988-1993 event was the longest of the three major droughts and consequently had the
555 greatest drought magnitude. The groundwater and meteorological droughts start
556 approximately contemporaneously in the winter of 1988. In CL2 the drought was continuous
557 with negative SGI from November 1988 to November 1993, whereas in CL4 there were two
558 short breaks in the drought and numerous breaks in the drought in CL1. In CL2 there was a
559 gradual intensification in the drought magnitude across the event, peaking in June 1992 at an
560 SGI of -1.85 (four months after the peak SPI_{12} meteorological drought). In contrast, not only
561 were there short breaks in the drought in CL1 and CL4 but there were approximately annual
562 cycles of drought intensification and decline over the four year period – these were
563 particularly pronounced in CL4. This is seen in Fig. 9a where between 1988 and 1993 the
564 drought status of CL4 is designated by the red tones in the heatmap, but that these tones show
565 a series of approximately annual variations giving the appearance of vertical stripes during
566 that period and within that cluster. However, the most pronounced differences in response to
567 major droughts between clusters CL1, CL2 and CL4 is in the timing of the end of drought.
568 Groundwater drought conditions ended in CL1 and CL4 in May 1993, seven months after the
569 end of the meteorological drought, but this was still six months before the groundwater
570 drought ended in CL2 (Fig. 9a).

571 The 1995 to 1997 drought, although shorter than the 1988 to 1993 drought, followed a similar
572 pattern with groundwater drought starting approximately contemporaneously with the
573 meteorological drought. Although it was a continuous event for all three clusters (there were
574 no breaks in the drought for CL1 and CL4), CL1 and CL4 again show approximately annual

575 intensifications and declines in drought status during the episode. Such approximately annual
576 changes in drought status are not seen in CL2. The 1995 to 1997 drought had the greatest
577 magnitude in CL2 due to the prolonged end to the drought in this cluster, with groundwater
578 drought in CL1 and CL4 finishing approximately contemporaneously with the meteorological
579 drought but six months later in CL2. The 2011 to 2012 drought was much shorter than the
580 other two multi-annual droughts, lasting just over a year starting relatively abruptly in early
581 2012 and finished abruptly in CL1 and CL4 in May 2012 in response to an unusual episode
582 of spring recharge Parry et al. (2013). The groundwater drought in CL2 again finished
583 relatively late, this time about three months later, in August 2012. The relatively short delay
584 in the breaking of the groundwater drought in CL2 compared with CL1 and CL4 probably
585 reflects the relatively smaller groundwater drought deficit accumulated due to the shorter
586 duration and lower magnitude of the drought compared with the 1988 to 1993 and 1995 to
587 1998 drought episodes.

588

589 **5. Discussion**

590 The results of the regional analysis of droughts based on cluster analysis are consistent with
591 current conceptualisations of the dynamics of drought in hydrological systems. Propagation
592 of drought through catchments and in particular through the groundwater compartment is
593 well documented (Peters et al., 2003; 2006; Tallaksen et al., 2006) and four components of
594 drought propagation are recognised, i.e. pooling, attenuation, lag and lengthening, three of
595 which (attenuation, lag and lengthening) are associated with modifications of drought signals
596 in groundwater (Van Loon, 2015). Attenuation results in smoothing of the maximum drought
597 anomaly, lag describes the delay in the onset of the drought signal as it passes through the
598 hydrological cycle (for example, see Fig. 3a and Fig. 4 of Van Loon, 2015.), and lengthening
599 extends the period of drought. Considering Table 3 that summarises the three multi-annual
600 droughts and comparing event magnitude for SPI₁₂, CL1 CL2 and CL4 respectively, there is,
601 as would be expected, evidence of a general attenuation of the SPI drought signal in the three
602 clusters compared with SPI₁₂. Lagging of the multi-annual groundwater droughts behind
603 meteorological droughts is not so easy to unambiguously quantify. Clearly the nature and
604 degree of the lag is sensitive to the rainfall accumulation period used to define the
605 meteorological drought index most closely correlated with SGI. In the present case,
606 accumulation periods of 4, 16, and 9 months are required for CL1, 2 and 4 respectively to
607 achieve optimal correlation between the SPI and SGI time series. Finally, the results of the

608 present study strongly support the concept of lengthening of groundwater drought relative to
609 meteorological drought (Van Loon, 2015). The results demonstrate that lengthening is most
610 pronounced following longer and deeper groundwater droughts. They serve to emphasise that
611 there can be significant differences in the lengthening response between different clusters,
612 even within with the same aquifer. It also appears that the degree of lengthening may also be
613 related to SGI autocorrelation (the greatest degree of lengthening is observed in cluster CL2
614 associated with the largest SGI autocorrelation, m_{\max}).

615 The results of the regional analysis add to our current understanding of the controls on
616 groundwater droughts. Bloomfield and Marchant (2013) investigated how unsaturated zone
617 thickness and the hydraulic diffusivity of aquifers may relate to m_{\max} . Using 14 SGI time
618 series from four different aquifers around the UK (including one site from the Lincolnshire
619 Limestone and nine sites on the Chalk, although none from the present study) they found that
620 m_{\max} was broadly an inverse function of log hydraulic diffusivity, $\log D_{\text{diff}}$ (where D_{diff} is
621 given by T/S and where T is aquifer transmissivity and S is specific storage of the aquifer).
622 Although they also noted that when fractured aquifers, such as the Lincolnshire Limestone
623 and the Chalk that have similarly high hydraulic diffusivities, were specifically considered
624 there is no clear relationship between m_{\max} and $\log D_{\text{diff}}$. However, they did find a positive
625 relationship between unsaturated zone thickness and m_{\max} for fractured aquifers such as the
626 Chalk and Lincolnshire Limestone. Based on this observation, they proposed that unsaturated
627 zone drainage and recharge processes were an important contributory factor in determining
628 autocorrelation or ‘memory’ in groundwater level hydrographs and by inference an
629 influential factor on groundwater drought characteristics, particularly in fracture aquifer
630 systems. Here we investigate if a similar relationship between m_{\max} and unsaturated zone
631 thickness holds for CL1, CL2 and CL4, clusters dominated by fractured aquifers.

632 Figure 12 shows box plots of unsaturated zone thickness for CL1, CL2 and CL4 as a function
633 of m_{\max} for each cluster (where unsaturated zone thickness is taken as the mean depth to
634 groundwater recorded for sites in each cluster over the study period). In addition,
635 corresponding observations for ten boreholes in fractured aquifers from Bloomfield and
636 Marchant (2013) are also shown for reference. The results of the present study are consistent
637 with those of Bloomfield and Marchant (2013, Fig. 13a) and show: increasing mean
638 unsaturated zone thickness with increasing cluster m_{\max} ; increasing variability in unsaturated
639 zone thickness with increasing cluster m_{\max} ; and increasing maximum unsaturated zone
640 thickness with increasing cluster m_{\max} . Bloomfield and Marchant (2013) previously noted that

641 such observations are consistent with the findings of Peters et al. (2005), since unsaturated
642 zone thickness is a function of distance to streams. However, in the present study area (Fig.
643 1) surface drainage is virtually absent from the northern Lincolnshire Limestone that
644 dominates CL1 and is limited over both the Chalk (CL2) and the southern Lincolnshire
645 Limestone (CL4). Instead we postulate that unsaturated zone thickness, and hence m_{\max} , is
646 affected by more general catchment characteristics such as extent of outcrop, topography,
647 intrinsic aquifer characteristics and aquifer thickness that all influence, through unsaturated
648 zone drainage and saturated flow processes, the overall shape of the piezometric surface in
649 the aquifers. For example, of the three aquifers in the study region the Chalk has the most
650 extensive outcrop; it is the thickest aquifer, up to five times thicker than the Lincolnshire
651 Limestone; and forms hills up to ~150 m asl compared to hills about 70 m asl across the
652 southern Lincolnshire Limestone, while it is associated (CL2) with the largest m_{\max} and the
653 longest and highest magnitude droughts. As such, the relationships between unsaturated zone
654 thickness, SGI autocorrelation and hence groundwater drought characteristics are not trivial
655 and appear to reflect a number of fundamental catchment properties and processes that effect
656 groundwater level dynamics and hence groundwater drought phenomena.

657 Although clustering of groundwater hydrographs is not novel in itself (Winter, 2000; Moon et
658 al, 2004; Upton and Jackson, 2011) this is the first time these techniques have been
659 systematically applied to investigate groundwater droughts. The approach described is
660 generic and widely applicable and here we briefly highlight some of the methodological
661 considerations, and implications for monitoring and prediction of groundwater droughts. The
662 *k*-means clustering has been performed on the complete SGI hydrographs, including periods
663 of relatively high groundwater level stand, even though the aim of the hydrograph
664 classification has been to investigate regional variations in groundwater droughts. Yet the
665 resulting clusters have been shown to effectively identify distinct regional groundwater
666 drought responses across the study area. For example, they reflect the major drought history
667 across the study region (Fig. 2 and Fig. 7), and identify spatially coherent hydrographs that
668 are consistent with know hydrogeological differences across the study area (Fig. 3c and Fig.
669 9a). Eltahir and Yeh (1999) investigated the asymmetry of groundwater hydrographs to high
670 and low groundwater level stands and noted that ‘droughts leave a significantly more
671 persistent signature on groundwater hydrology than floods’. They inferred that this
672 phenomenon was because discharge of groundwater to streams is an efficient dissipation
673 mechanism for wet anomalies and that this discharge is often strongly nonlinear. This may

674 explain, at least in part, why the hydrograph classification scheme based on full hydrographs
675 provides such a good basis for analysis of the heterogeneous response of groundwater to
676 drought at the regional scale. However, there is potential for future work to investigate if the
677 hydrograph classification can be improved by focussing on, or giving more weight to
678 episodes of drought in the SGI time series.

679 In addition to identifying three clusters of SGI hydrographs, CL1, CL2 and CL4, that exhibit
680 different characteristic responses to meteorological drivers, the *k*-means clustering also
681 identified three relatively small clusters of SGI hydrographs, CL3, CL5 and CL6, where there
682 were either: trends in the SGI time series; temporal anomalies expressed as anomalous phase
683 relationships between cluster SGI and the regional SGI time series; or relatively poor
684 coherency in SGI time series with a given cluster. In these three clusters it has been inferred
685 that hydrographs may have been variably impacted by anthropogenic factors, such as
686 groundwater abstraction. Although the CA was not specifically designed to identify
687 anthropogenically impacted groundwater hydrographs the classification scheme could be
688 used to that end since it can differentiate between clusters showing trends superimposed on
689 the regional signals (e.g. CL3 and CL5) and clusters with anomalous phase relationships with
690 the regional signal (e.g. CL6). The presence of a trend in a cluster of hydrographs may be
691 indicative of an anthropogenic impact, for example from unsustainable abstraction (declining
692 trend) or from groundwater rebound (rising trend). Where there is limited prior information
693 regarding groundwater withdrawals across a region, a not uncommon situation in areas where
694 abstraction is not highly regulated, cluster analysis could be used, either as it has been in the
695 present study based on a set of heuristic rules to identify a suitable number of clusters, or in
696 an exploratory manner. If it is used in a more exploratory manner, either hierarchical or non-
697 hierarchical clustering could be undertaken and then clusters searched to identify spatially
698 coherent clusters that show significant downward trends in hydrographs (where significance
699 of trends in a cluster could be tested and quantified using standard tests, such as Mann-
700 Kendall and Sen's slope estimates). Any spatial coherence in clusters exhibiting downward
701 trends may be taken as indicating the presence of potentially unsustainable abstraction. For
702 the purposes of a study where the stationarity of the data is important, if trends in individual
703 hydrographs are already known then either these hydrographs can be removed from an
704 analysis or the trends could be identified and removed prior standardisation and clustering of
705 the hydrographs.

706 It has been shown that there can be pronounced differences in the characteristics of multi-
707 annual drought episodes between aquifers within a region (Fig. 9a). During multi-annual
708 droughts some clusters temporarily go out of drought conditions while others will continually
709 show deepening drought conditions over two or more years, and some clusters stay in
710 groundwater drought for many months after groundwater (and meteorological) drought has
711 ceased in other clusters. If observations such as these or similar can be made for a region they
712 may have important implications for monitoring groundwater droughts and water resource
713 management in multi-aquifer (cluster) systems. For example, at the end of a drought, sites in
714 more quickly responding clusters may act as leading indicators of the end of groundwater
715 drought at sites in more slowly responding clusters. In addition to the implications for
716 groundwater monitoring particularly during long droughts, if there is sufficient understanding
717 of regional variations in groundwater responses (i.e. relative differences in the timing and
718 intensity of groundwater drought between different aquifers in a region or between sub-
719 regions within an aquifer), then this understanding could be used to inform appropriate
720 groundwater water resource management strategies and so may enable some of the worst
721 impacts of the groundwater drought to be mitigated.

722 More generally we see a range of possible benefits to clustering groundwater hydrographs.
723 For example, ‘sentinel’ boreholes within each cluster, those that are closest to the mean
724 behaviour of a group, could be identified and used as indicative of the groundwater response
725 of a wider area. Missing data is a common issue with groundwater hydrographs, and
726 clustering techniques could potentially be used to identify suitable boreholes from which
727 groundwater levels could be infilled. However, more importantly, clustering could be used in
728 combination with groundwater models to aid the prediction of groundwater droughts. A range
729 of techniques can be used to model groundwater hydrographs at a site, i.e. non-distributed
730 groundwater models, including statistical models (Ahn 200; Bloomfield et al. 2003), artificial
731 neural network models (Sreekanth et al. 2009) and ‘black box’ models (Mackay et al, 2014).
732 The hydrograph cluster analysis could be used in combination with any of these techniques
733 for groundwater drought prediction. For example, groundwater level prediction 1 to 12
734 months out is currently undertaken in the UK for selected sites using a black-box, lumped
735 parameter model (Jackson et al. 2013; Mackay et al. 2014; Hydrological Outlooks, 2015)
736 driven by probabilistic estimates of future rainfall. Regional inferences of future groundwater
737 levels are then based on qualitative interpretations of the individual sites. Applying similar
738 predictive modelling systems to mean cluster hydrographs that are representative of spatially

739 coherent regions of groundwater drought response instead of individual site specific
740 hydrographs could enable a more rigorous prediction of the spatial distribution of future
741 groundwater droughts.

742 **6. Conclusions**

743 Cluster analysis (CA) when applied to SGI time series of consistent length for multiple sites
744 across a region has been shown to provide a robust approach to the regional analysis of
745 groundwater droughts. In the present study an agglomerative hierarchical complete-linkage
746 strategy and a *k*-means clustering strategy were tested. The *k*-means clustering was found to
747 be most suitable. However, for any given case study a range of non-hierarchical algorithms
748 and hierarchical classification schemes should be explored to see which is most appropriate.

749 A heuristic, rule-based approach was found useful in guiding the selection of the optimal
750 number of clusters, where the rules applied prior knowledge of the hydrogeology of the study
751 area including information related to spatial variations in catchment and aquifer
752 characteristics. For the present case study, both non-hierarchical algorithms and hierarchical
753 classification schemes provide better clustering of SGI time series than a simple three-fold
754 classification simply based on geology alone, with the *k*-means clustering providing the best
755 clustering. Membership of the resulting *k*-means clusters is shown to be dominated by
756 hydrogeological factors and the effect of heterogeneity in precipitation over the study area on
757 cluster composition is inferred to be negligible.

758 The clusters successfully discriminate different responses to groundwater drought both in
759 terms of drought metrics for the complete time series and with respect to the detailed
760 response of sites in each cluster during specific major episodes of multi-annual drought.
761 Groundwater drought characteristics can be linked, through the autocorrelation structure of
762 cluster hydrographs, to the distribution of unsaturated zone thickness. This reflects the role of
763 a range of catchment and aquifer properties and processes that influence groundwater level
764 dynamics, including topography, aquifer thickness and extent of outcrop, unsaturated zone
765 drainage characteristics and saturated groundwater flow.

766 This approach to groundwater hydrograph clustering is flexible, can be applied in a wide
767 range of hydrogeological settings where suitable hydrographs are available, and enables
768 spatially variable responses of groundwater to drought to be quantified.

769

770 **Acknowledgements**

771 We would like to thank Henry Holbrook with help in preparation of the figures. The work
772 described has been funded by the British Geological Survey (Natural Environment Research
773 Council), and this paper is published with the permission of the Executive Director of the
774 British Geological Survey (Natural Environment Research Council).

775

776 **References**

777 Ahn, H.: Modelling groundwater heads based on second-order difference time series models.
778 *Journal of Hydrology*, 234, 82-94, 2000.

779 Allen, D. J., Brewerton, L. J., Coleby, L. M., Gibbs, B. R., Lewis, M. A., MacDonald, A. M.,
780 Wagstaff, S. J., and Williams, A. T.: The physical properties of major aquifers in England
781 and Wales, British Geological Survey Research Report WD/97/34, Keyworth, UK, 1997.

782 Bloomfield, J. P.: Characterisation of hydrogeologically significant fracture distributions in
783 the Chalk: An example from the Upper Chalk of southern England, *Journal of Hydrology*,
784 184, 335-379, 1996.

785 Bloomfield, J. P., and Marchant, B. P.: Analysis of groundwater drought building on the
786 Standardised Precipitation Index approach, *Hydrology and Earth System Sciences*, 17, 4769-
787 4787, 2013.

788 Bloomfield, J. P., Brewerton, L.J, and Allen, D.J.: Regional trends in matrix porosity and dry
789 density of the chalk of England, *Quarterly Journal of Engineering Geology*, 28, S131-S142,
790 1995.

791 Bloomfield, J.P., Gaus, I., and Wade, S.D.: A method for investigating potential impacts of
792 climate change scenarios on annual minimum groundwater levels. *Water and Environment*
793 *Journal*, 17, 86-91, 2003.

794 Bonaccorso, B., Bordini, A., Cancelliere, A., Rossi, G., and Sutera, A.: Spatial variability of
795 drought: An analysis of the SPI in Sicily, *Water Resource Management*, 17, 273-296, 2003.

796 Chang, T. J. and Teoh, C. B.: Use of the kriging method for studying characteristics of
797 ground water droughts, *Journal of the American Water Resources Association*, 31, 1001-
798 1007, 1995.

799 Dore, A. J., Kryza, M., Hall, J. R., Hallsworth, S., Keller, V. J. D., Vieno, M., and Sutton, M.
800 A.: The influence of model grid resolution on estimation of national scale nitrogen deposition
801 and exceedance of critical loads, *Biogeosciences*, 9, 1597-1609, 2012

802 Eder, B. K., Davis, J. M., and Monahan, J. F.: Spatial and temporal analysis of the Palmer
803 drought severity index over south-eastern United States, *Journal of Climatology*, 7, 31-51,
804 1987.

805 Eltahir, E. A. B., and Yeh, P. J-F.: On the asymmetric response of aquifer water level to
806 floods and droughts in Illinois, *Water Resources Research*, 35, 1199-1217, 1999.

807 Environment Agency. 2014. National groundwater level database for England, Environment
808 Agency. <http://data.gov.uk/data> last retrieved 26 August 2014.

809 Fleig, A. K., Tallaksen, L. M., Hisdal, H., and Hannah, D. M.: Regional hydrological drought
810 in north-western Europe: Linking a new regional drought area index with weather types,
811 *Hydrological Processes*, 25, 1163-1179, 2011.

812 Folland C.K., Hannaford, J., Bloomfield J.P., Kendon, M., Svensonn, C., Marchant, B.P.,
813 Prior, J., and Wallace, E. Multi-annual droughts in the English Lowlands: a review of their
814 characteristics and climate drivers in the winter half year, *Hydrology and Earth Systems
815 Sciences*, 19, 2353-2375, 2015.

816 Hannaford, J., Lloyd-Hughes, B., Keef, C., Parry, S., and Prudhomme, C.: Examining the
817 large-scale spatial coherence of European drought using regional indicators of precipitation
818 and streamflow deficit, *Hydrological Processes*, 25, 1146-1162, 2011.

819 Hannah, D. M., Smith, B. P. G., Gurnell, A. M., and McGregor, G. R.: An approach to
820 hydrograph classification, *Hydrological Processes*, 14, 317-338, 2000.

821 Hisdal, H., and Tallaken, L. M.: Estimation of regional meteorological and hydrological
822 drought characteristics, *Journal of Hydrology*, 281, 230-247, 2003.

823 Hydrological Outlooks. 2015. <http://www.hydoutuk.net> last downloaded 25th August 2015

824 Jackson, C. R., Pachocka, M., and Mackay, J. D: Hydrological outlook: outlook based on
825 modelled groundwater levels and associated climate forecasts. British Geological Survey
826 Report OR/13/046, Nottingham, UK. 2013. <http://nora.nerc.ac.uk/503966/> last downloaded
827 25 August 2015

828 Jones, H. K., Morris, B. L., Cheney, C. S., Brewerton, L. J., Merrin, P. D., Lewis, M. A.,
829 MacDonald, A. M., Coleby, L. M., Talbot, J. C., McKenzie, A. A., Bird, M. J., Cunningham,
830 J. and Robinson, V. K.: The physical properties of minor aquifers in England and Wales,
831 British Geological Survey Technical Report, WD/00/4, Keyworth, UK, 2000.

832 Karl, R. T., and Koscieny, A. J.: Drought in the United States:1895-1981, *Journal of*
833 *Climatology*, 2, 313-329, 1982.

834 Keller, V., Young, A. R., Morris, D., and Davies, H.: Continuous Estimation of River Flows
835 (CERF), Technical Report: Estimation of Precipitation Inputs, Environment Agency R&D
836 Project Report WD-101, Centre for Ecology and Hydrology, Wallingford, 2005.

837 Kendon, M., Marsh, T. J., and Parry, S.: The 2010-2012 drought in England and Wales,
838 *Weather*, 68, 88-95, 2013

839 Kingston, D. C., Flieg, A. K., Tallaksen L. M., and Hannah, D. M.: Ocean-atmosphere
840 forcing of summer streamflow droughts in Great Britain, *American Meteorological Society*,
841 14, 331-344, 2013

842 Klugman, M. R.: Drought in the Upper Midwest, 1931-1969, *Journal of Applied*
843 *Meteorology*, 17, 1425-1431, 1978.

844 Lana, X., Serra, C., and Burgueno, A.: Patterns of monthly rainfall shortage and excess in
845 terms of the standardised precipitation index for Catalonia (NE Spain). *International Journal*
846 *of Climatology*, 21, 1669-1691, 2001.

847 Lloyd-Hughes, B., and Saunders, M. A.: A drought climatology for Europe, *International*
848 *Journal of Climatology*, 22, 1571-1592, 2002.

849 Lloyd-Hughes, B., Prudhomme, C., Hannaford, J., Parry, S., Keef, C., and Rees, H. G.:
850 Drought catalogues for UK and Europe. Environment Agency Science Report,
851 SC070079/SR, Environment Agency, Bristol, 2010.

852 Lorenzo-Lacruz, J., Moran-Tejeda, E., Vincente-Serrano, S. M., and Lopez-Moreno, J. I.:
853 Streamflow droughts in the Iberian Peninsula between 1945 and 2005: spatial and temporal
854 patterns, *Hydrology and Earth System Sciences*, 17, 119-134, 2013.

855 Mackay, J.D., Jackson, C.R., and Wang, L. A lumped parameter conceptual model to simulate
856 groundwater level time series. *Environmental Modelling software*, 61, 229-245. 2014

857 Marsh, T. J., and Hannaford, J.: UK Hydrometric Register, Hydrological data UK series,
858 Centre for Ecology and Hydrology, Wallingford, 2008.

859 Marsh, T. J., Cole, G., and Wilby, R.: Major droughts in England and Wales. 1800-2006,
860 *Weather*, 62, 87-93, 2007.

861 Marsh, T. J., Simon, P., Kendon, M., and Hannaford, J.: The 2010-12 drought and subsequent
862 extensive flooding: a remarkable hydrological transformation, Centre for Ecology &
863 Hydrology, Wallingford, 54pp, 2013.

864 Maurice, L. D., Atkinson, T. C., Barker, J. A., Bloomfield, J. P., Farrant, A. R., and Williams,
865 A. T.: Karstic behaviour of groundwater in the English Chalk, *Journal of Hydrology*, 330, 63-
866 70, 2006.

867 McKee, T. B., Doesken, N. J., and Leist, J.: The relationship of drought frequency and
868 duration time scales, 8th Conference on Applied Climatology, Anaheim, California, 17 to 22
869 January 1993, 179-184, 1993.

870 Mendicino, G., Senatore, A., and Versace, P.: A Groundwater Resource Index (GRI) from
871 drought monitoring and forecasting in a Mediterranean climate, *Journal of Hydrology*, 357,
872 282-302, 2008.

873 Mishra, A. K., and Singh, V. P.: A review of drought concepts, *Journal of Hydrology*, 391,
874 202-216, 2010.

875 Moon, S. K., Woo, N. C., and Lee, K. S.: Statistical analysis of hydrographs and water-table
876 fluctuation to estimate groundwater recharge, *Journal of Hydrology*, 292, 1989-209, 2004.

877 Parry, P., Marsh, T., Kendon, M.: 2012: from drought to floods in England and Wales,
878 *Weather*, 68, 268-274. 10.1002/wea.2152, 2013

879 Peters, E., Torfs, P. J. J. F., Van Lanen, H. A. J., and Bier, G.: Propagation of drought
880 through groundwater – a new approach using linear reservoir theory, *Hydrological Processes*,
881 17, 3023-3040, 2003.

882 Peters, E., Van Lanen, H. A. J., Torfs, P. J. J. F., and Bier, G.: Drought in groundwater –
883 drought distribution and performance indicators, *Journal of Hydrology*, 306, 302-317, 2005.

884 Peters, E., Bier, G., Van Lanen, H. A. J., and Torfs, P. J. J. F.: Propagation and spatial
885 distribution of drought in a groundwater catchment, *Journal of Hydrology*, 321, 257-275,
886 2006.

887 Raziel, T., Bordi, I., and Pereira, L. S.: A precipitation-based regionalisation for Western Iran
888 and regional drought variability, *Hydrology and Earth System Sciences*, 12, 1309-1321,
889 2008.

890 Sadri, S and Burn, D. D.: Copula-based pooled frequency analysis of droughts in the
891 Canadian Praries, *Journal of Hydrological Engineering*, 19, 277-289, 2014.

892 Santos, J. F., Pulido-Calvo, I., and Portela, M. M.: Spatial and temporal variability of
893 droughts in Portugal, *Water Resources Research*, 46, W03503, 2010.

894 Stahl, K., and Demuth, S.: Linking streamflow drought to the occurrence of atmospheric
895 circulation patterns, *Hydrological Sciences Journal*, 44, 467-482, 1999.

896 Stahl, K., and Demuth, S.: Regional classification. In: Demuth, S. Stahl, K. (Eds.) *ARIDE –*
897 *Assessment of the Regional Impact of Drought in Europe*, Institute of Hydrology, University
898 of Freiburg, Frieburg, Germany, pp. 98-105, 2001.

899 Sreekanth, P.D., Geethanjali, N, Sreedevi, P.D., Ahmed, S., Ravi Kumar, N., and Kamala
900 Jayanthi, P.D.: Forecasting groundwater levels using neural networks, *Current Science.*, 96,
901 933-939, 2009.

902 Tallaksen, L. M., and Van Lanen, H. A. J.: Hydrological drought. Processes and estimation
903 methods for streamflow and groundwater, *Developments in Water Sciences* 48, Elsevier,
904 Netherlands, 2004.

905 Tallaksen, L. M., Hisdal, H. And Van Lanen, H. A. J.: Propagation of drought in a
906 groundwater fed catchment, the Pang in UK. In Demuth, S. (Ed.), *FRIEND 2006 – Water*
907 *Resources Variability: Processes, Analyses and Impacts*, IAHS Publication 308, 128-133,
908 2006.

909 Tallaksen, L. M., Hisdal, H., and Van Lanen, H. A. J.: Space-time modelling of catchment
910 scale drought characteristics, *Journal of Hydrology*, 375, 363-372, 2009.

911 Upton, K. A. and Jackson, C. R.: Simulation of the spatio-temporal extent of groundwater
912 flooding using statistical methods of hydrograph classification and lumped parameter models,
913 *Hydrological Processes*, 25, 1949-1963, 2011.

914 Van Lanen, H.A.J.: On the definition of groundwater drought. *Geophysical Research*
915 *Abstract*, 7, 10867. 2005.

916 Van Lanen, H.A.J., and Peters, E.: Definition, effects and assessment of groundwater
917 droughts. In: Vogt, J.V. and Somma, F. (Eds.), *Drought and Drought Mitigation in Europe*,
918 Kulwer, Dordrecht, 49-61, 2000.

919 Van Lanen, H.A.J. and Tallaksen, L.M.. 2007. Hydrological drought, climate variability and
920 change, in: Climate and Water, edited by: Heinonen,M., Proceedings of the third
921 International Conference on Climate and Water, Helsinki, 3–6 September 2007, 488–493,
922 2007.

923 Van Lanen, H. A. J., Wanders, N., Tallaksen, L. M., and Van Loon, A. F.: Hydrological
924 drought across the world: impact of climate and physical catchment structure, *Hydrol. Earth*
925 *Syst. Sci.* 17: 1715–1732, doi:10.5194/hess-17-1715-2013, 2013.

926 Van Loon, A. F.: Hydrological drought explained, *WIREs Water*, doi:10.1002/wat2.1085,
927 2015.

928 Van Loon, A. F. and Laaha G.: Hydrological drought severity explained by climate and
929 catchment characteristics, *Journal of Hydrology*, 526, 3-14, 2015.

930 Van Loon, A. F. and Van Lanen, H. A. J.: A process-based typology of hydrological drought,
931 *Hydrol. Earth Syst. Sci.* 16: 1915-1946, doi:10.5194/hess-16-1915-2012, 2012.

932 Vicente-Serrano, S.M.: Spatial and temporal analysis of droughts in the Iberian Peninsula
933 [1910-2000]. *Hydrological Sciences Journal*, 51, 83-97, 2006.

934 Vicente-Serrano, S.M., and Cuadrat-Prats, J.M.: Trends in drought intensity and variability in
935 the middle Ebro valley (NE of the Iberian peninsula) during the second half of the twentieth
936 century. *Theoretical Applied Climatology*, 88, 247-258, 2007.

937 Webster, R. and Oliver, M.A.: *Statistical Methods in Soil and Land Resource Survey*. Oxford
938 University Press, U.K. 1990

939 Whitehead, E.J. and Lawrence, A.R.: The Chalk aquifer system of Lincolnshire. British
940 Geological Survey Research Report, RR/06/03, 2006. <http://nora.nerc.ac.uk/3699/>

941 World Meteorological Organization. Standardized Precipitation Index User Guide, WMO-
942 No. 1090, Geneva http://www.wamis.org/agm/pubs/SPI/WMO_1090_EN.pdf Last
943 downloaded, 13th August 2015

944

945 Table 1. Summary of features of the six *k*-means clusters.

946

Cluster	Number of sites				Statistic		
	Total	Lincolnshire Limestone	Spilsby Sandstone	Chalk	SPI/SGI maximum correlation	Representative accumulation period, q_{\max} (Months)	Autocorrelation range, m_{\max} (Months)
CL1	13	13	0	0	0.74	4	15
CL2	23	2	0	21	0.86	16	23
CL3	6	2	4	0	0.36	15	60
CL4	24	19	0	5	0.82	9	18
CL5	5	0	0	5	0.53	17	28
CL6	3	0	3	0	0.09	-	-
Total	74	36	7	31			

947

948

949

950 Table 2. Summary of drought event statistics for clusters C1, C2 and C4.

951

	CL1	CL2	CL4
Number of Drought events	39	15	18
Mean duration (months)	4.6	11.3	9.1
Maximum duration (months)	27	61	49
Mean event magnitude	-2.9	-7.9	-6.6
Mean event intensity	-0.43	-0.28	-0.4
Maximum event intensity	-1.1	-1.05	-1.13
No. events where $I < -1$	3	2	2

952

953

954

955 Table 3. Summary of the 1988-93, 1995-98 and 2011-12 drought events for clusters CL1,
 956 CL2 and CL4 (where D_{event} , M_{event} and I_{event} denote indices for drought event duration,
 957 magnitude and intensity respectively).

958

Drought episode	Drought index	Regional SPI ₁₂	Mean CL1	SGI CL2	Mean SGI CL4
1988 to 1993	Start date	Dec-88	Oct-88	Nov-88	Oct-88
	End date	Oct-92	May-93	Nov-93	May-93
	D_{event}	47	56	61	56
	M_{event}	-56.8	-37	-63.6	-41.6
	I_{event}	-1.2	-0.7	-1.0	-0.7
1995 to 1998	Start date	May-95	May-95	Aug-95	Jul-95
	End date	Oct-97	Jul-97	Feb-98	Aug-97
	D_{event}	30	27	31	26
	M_{event}	-34.3	-18.7	-32.4	-29.3
	I_{event}	-1.1	-0.7	-1.0	-1.1
2010 to 2012	Start date	Jan-11	May-11	Jan-11	Jul-10
	End date	Apr-12	May-12	Aug-12	May-12
	D_{event}	16	13	20	23
	M_{event}	-16.1	-13.9	-11.7	-21
	I_{event}	-1.0	-1.1	-0.6	-0.9

959

960

961

962

963 **Figure captions**

964

965 Figure 1. Case study area (left) and simplified geology map (right) showing locations of the
966 observation boreholes. Cross-section (bottom) illustrating the stratigraphic/depth
967 relationships between the three major aquifers in the study region: the Lincolnshire
968 Limestone, the Spilsby Sandstone and the Chalk.

969

970

971 Figure 2. a. SPI/SGI correlation as a heatmap, b. mean SPI₁₂ time series and c. mean SGI
972 time series for all 74 hydrographs.

973

974 Figure 3. a. cluster dendrogram for hierarchical classification ($k=6$) of SGI time series, b. map
975 showing the distribution of sites by clusters based on hierarchical classification ($k=6$), and c.
976 map showing the distribution of sites by clusters formed by k-means clustering ($k = 6$).

977

978 Figure 4. RMSSD as a function of the number of clusters for the hierarchical and non-
979 hierarchical k-means clustering algorithms and for a three-fold classification based on
980 geology alone.

981

982 Figure 5. Heatmaps of Pearson correlation between SGI and SPI for $q = 1$ to 36 months and
983 for lags up to 5 months. Maximum correlation is denoted by the closed black circles.

984

985 Figure 6. Mean SPI times series for each of the k-means clusters based on the accumulation
986 period q_{\max} for each cluster. Where the black line is SPI based on gridded precipitation series
987 for sites in a given cluster and the red line is SPI for the mean rainfall across the whole study
988 area based on the different aggregation periods, q_{\max} , for each cluster.

989

990 Figure 7. Mean SGI time series for each of the six k-means clusters.

991

992 Figure 8. Correlograms for each of the mean SGI time series (bold) and individual site time
993 series (grey) for each of the six k-means clusters showing variation in the autocorrelation
994 function (ACF) for lags up to 60 months.

995

996 Figure 9. Heatmaps showing a.) SGI varying with time for all 74 sites as function of the six
997 k-means clusters (left), and b.) correlations between all pairs of sites sorted as a function of
998 the six k-means clusters (right).

999

1000 Figure 10. Drought magnitude versus drought duration for sites in clusters CL1, CL2 and
1001 CL4.

1002

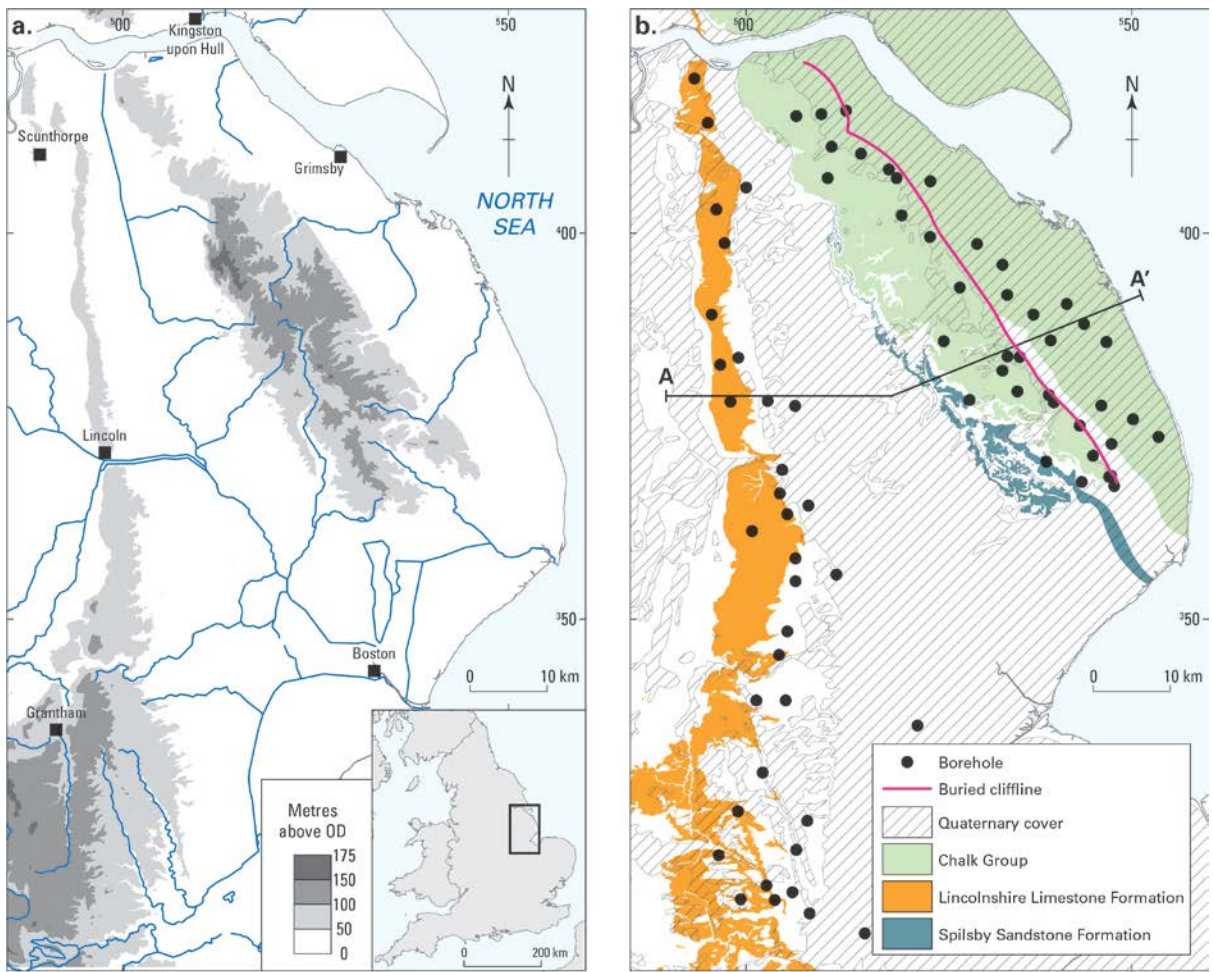
1003 Figure 11. Percentile plots of a. drought duration, b. drought magnitude, and c. drought
1004 intensity for clusters CL1, CL2 and CL4.

1005

1006 Figure 12. SGI autocorrelation (m_{\max}) as a function of unsaturated zone thickness.

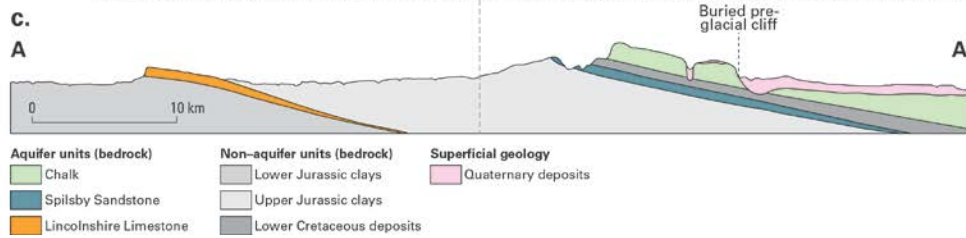
1007

1008 Figure 1.



Contains Ordnance Survey data © Crown Copyright and database rights 2014. Drainage networks and settlement locations Ordnance Survey data Crown Copyright, all rights reserved: 100021298

Geological data, BGS © NERC.



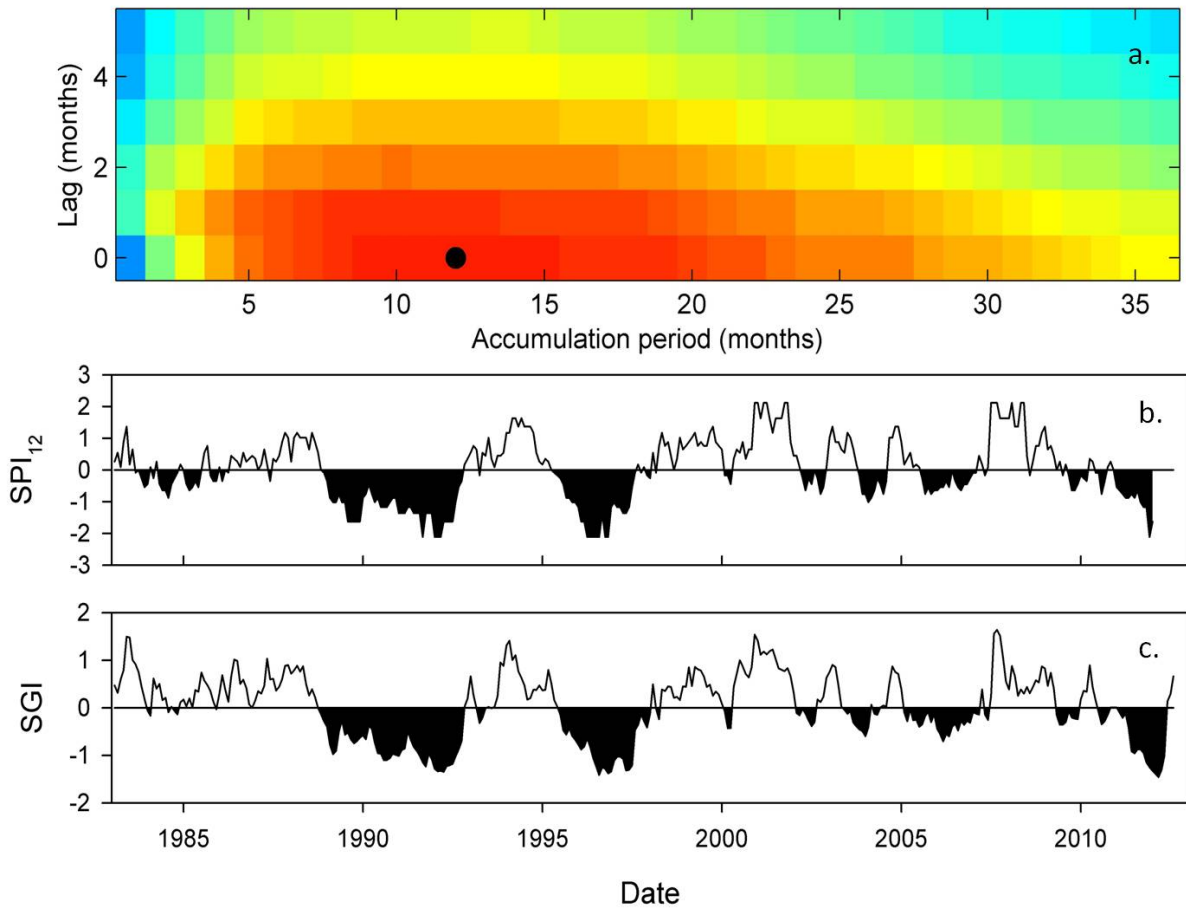
1009

1010

1011

1012

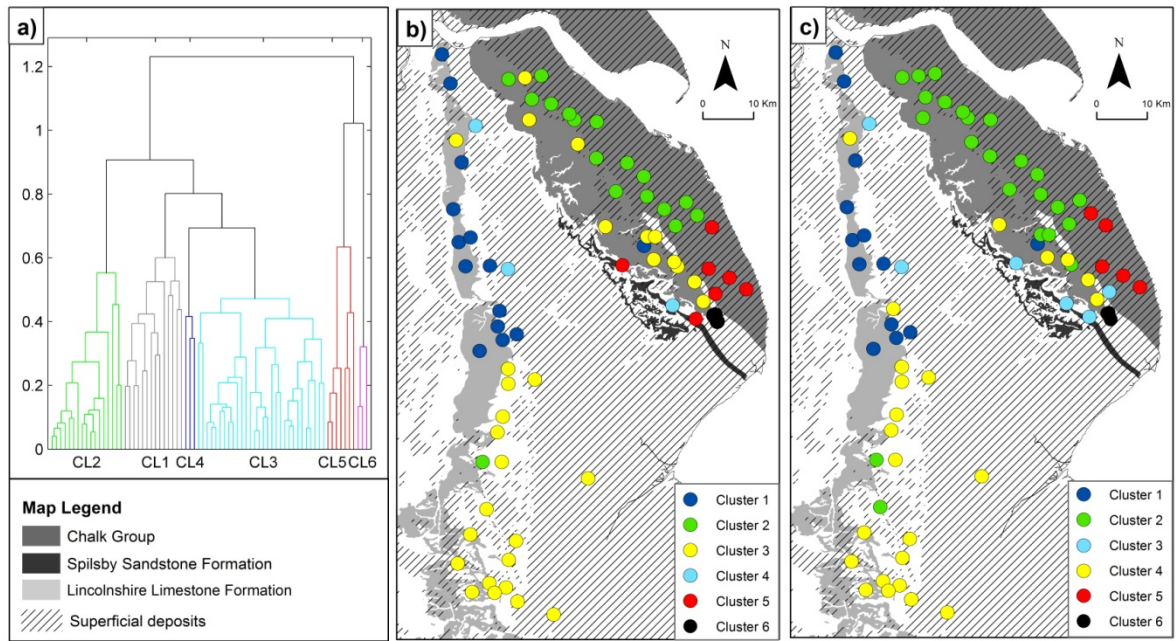
1013 Figure 2.



1014

1015

1016 Figure 3.

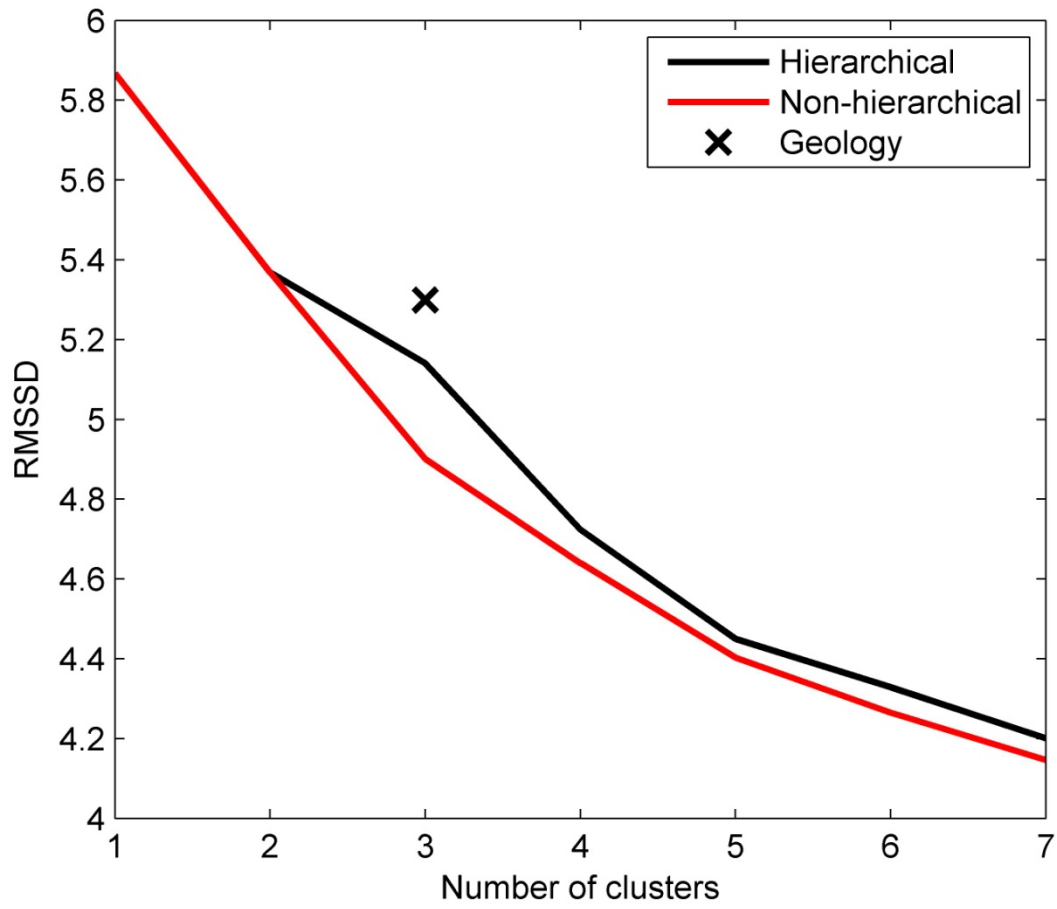


Geological data, BGS © NERC. Contains Ordnance Survey data © Crown copyright and database right (2014)

1017

1018

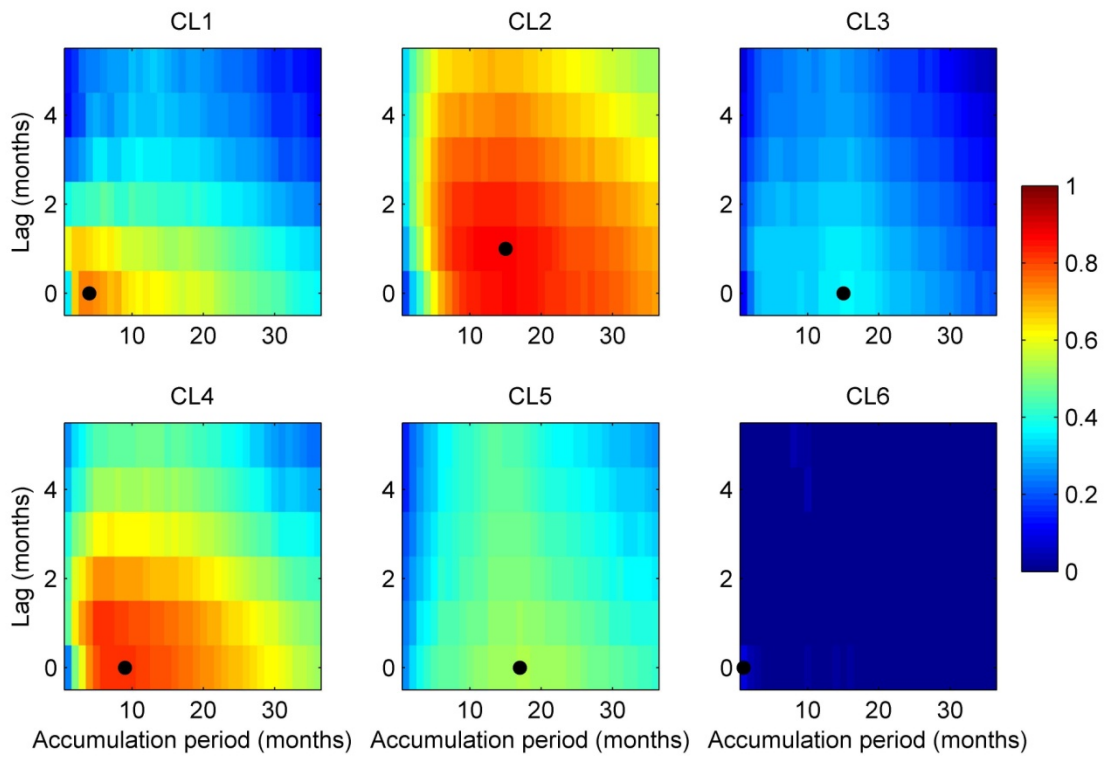
1019 Figure 4.



1020

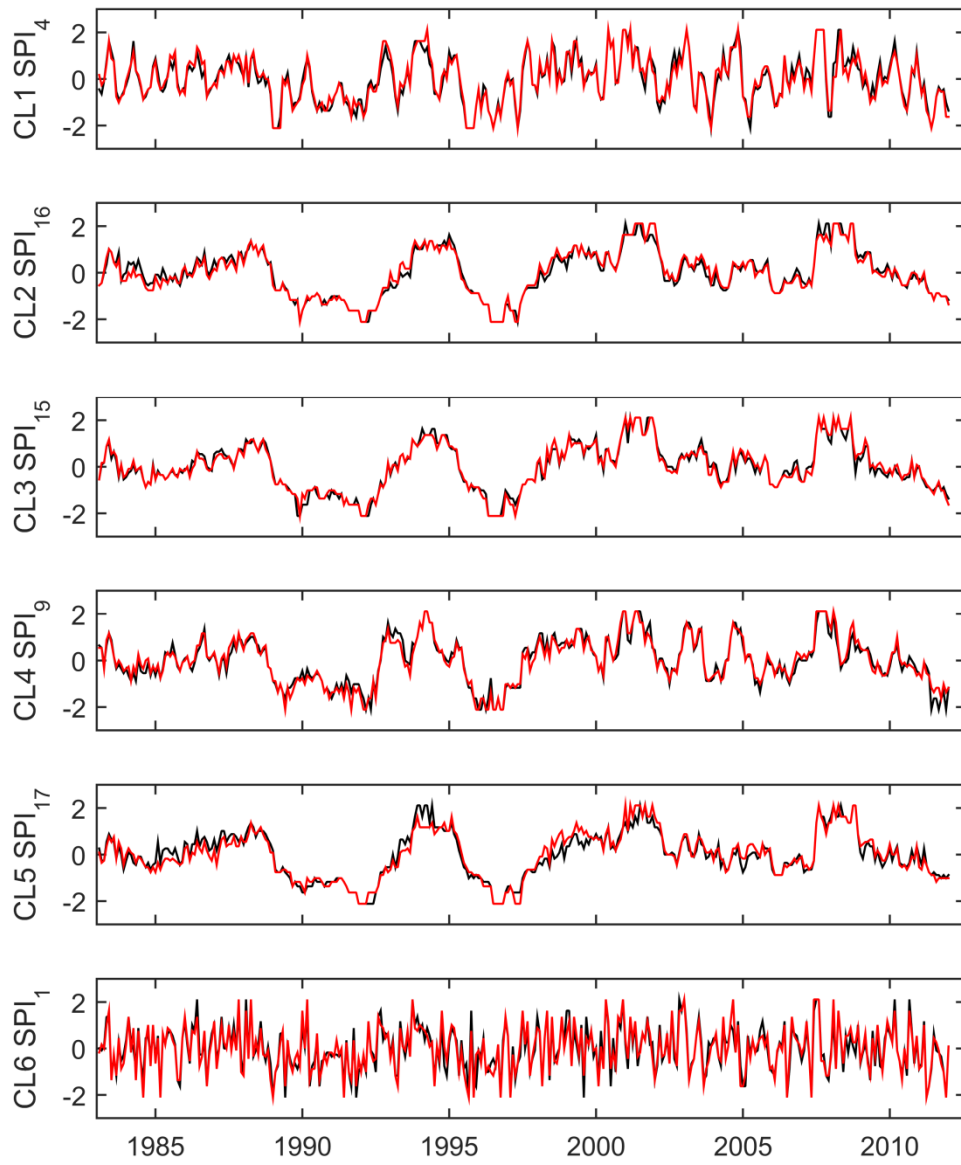
1021

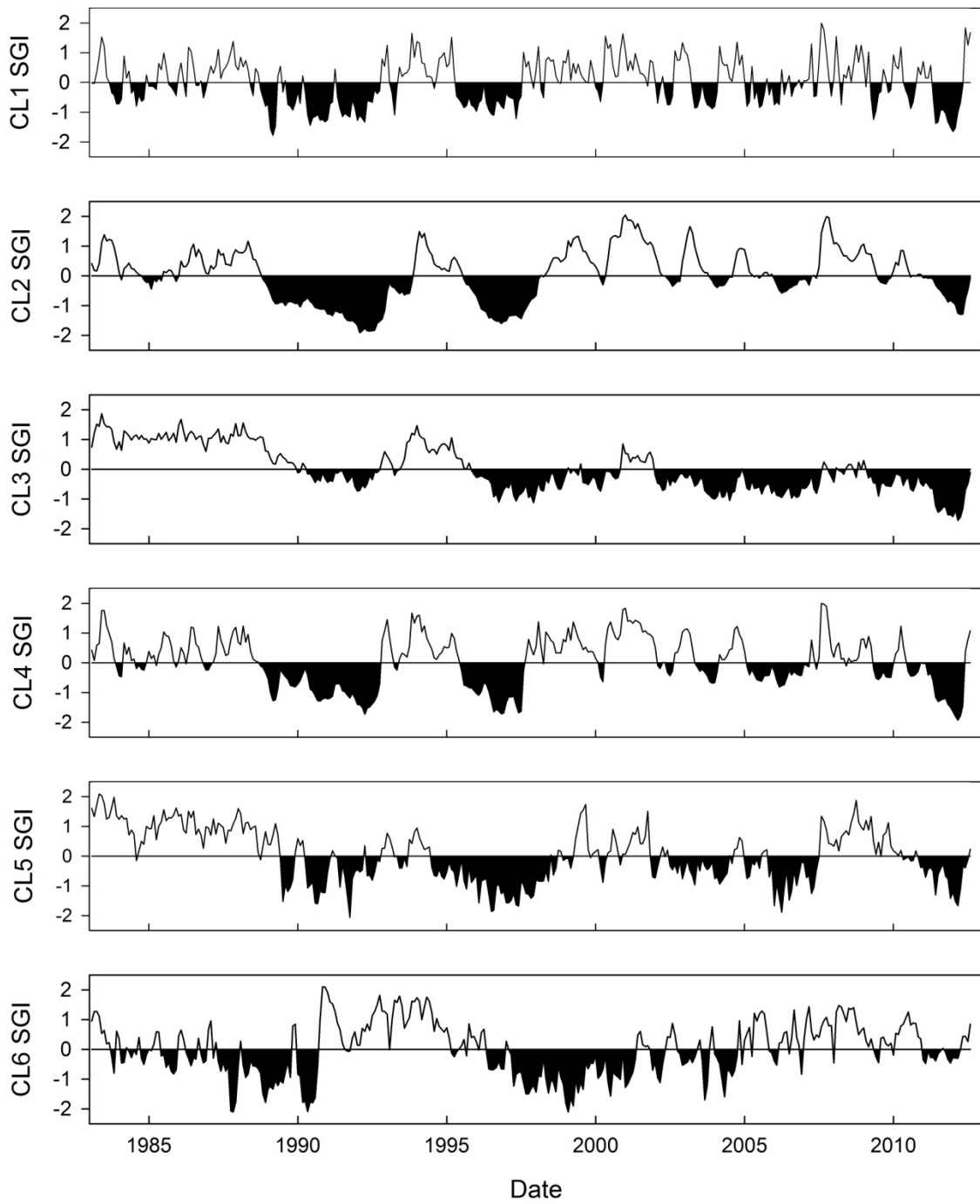
1022 Figure 5.



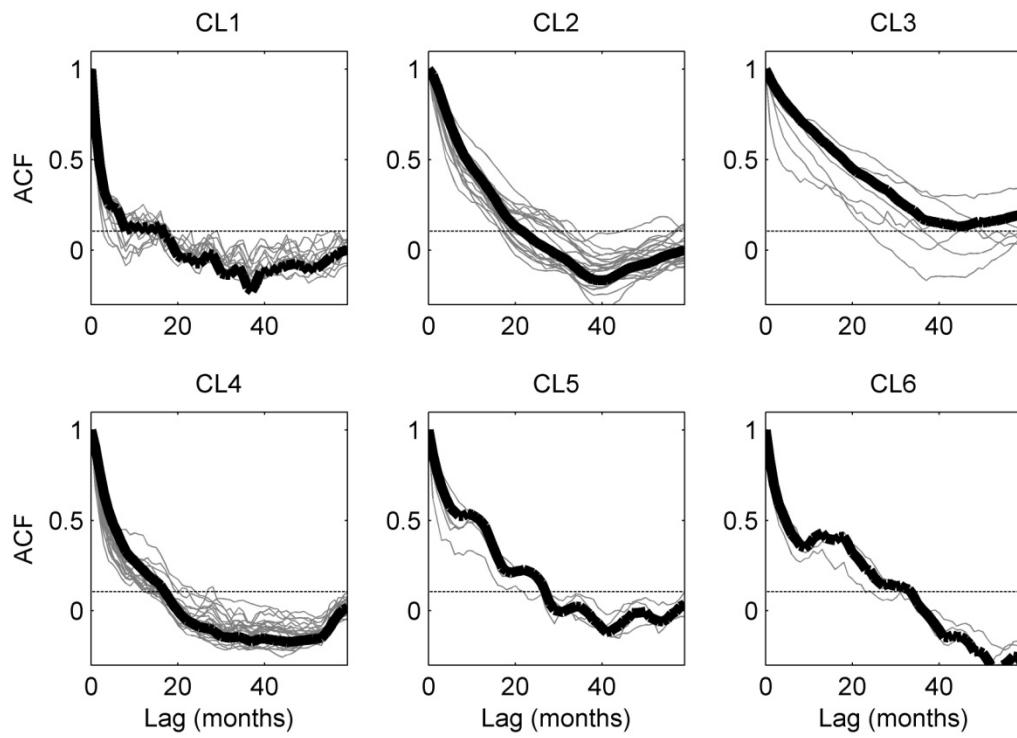
1023

1024



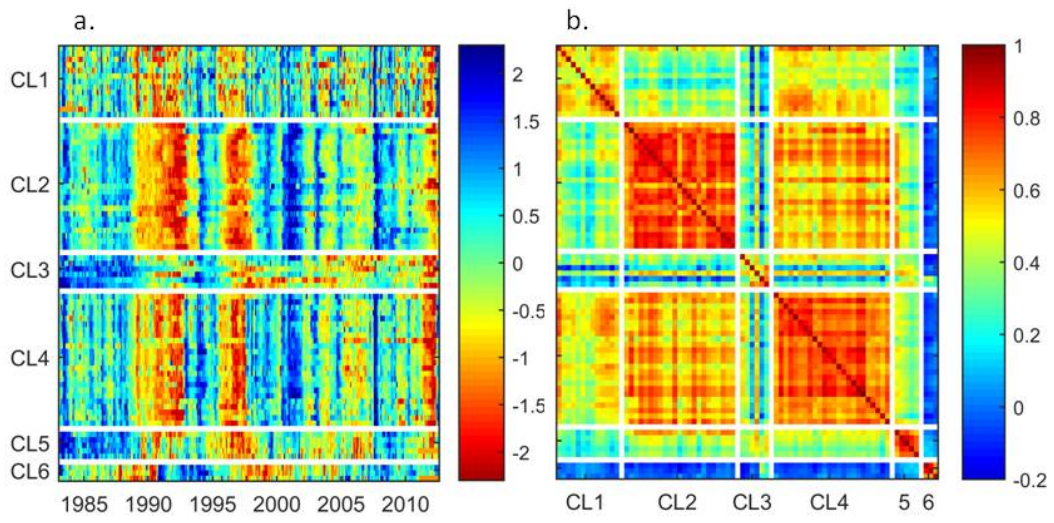


1031 Figure 8.

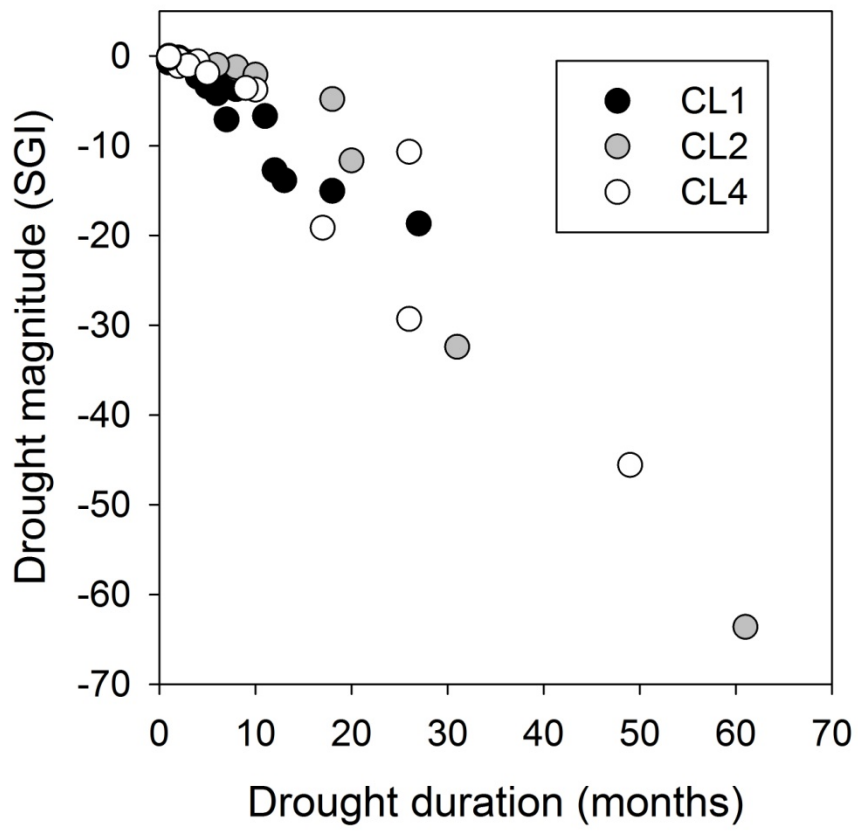


1032

1033



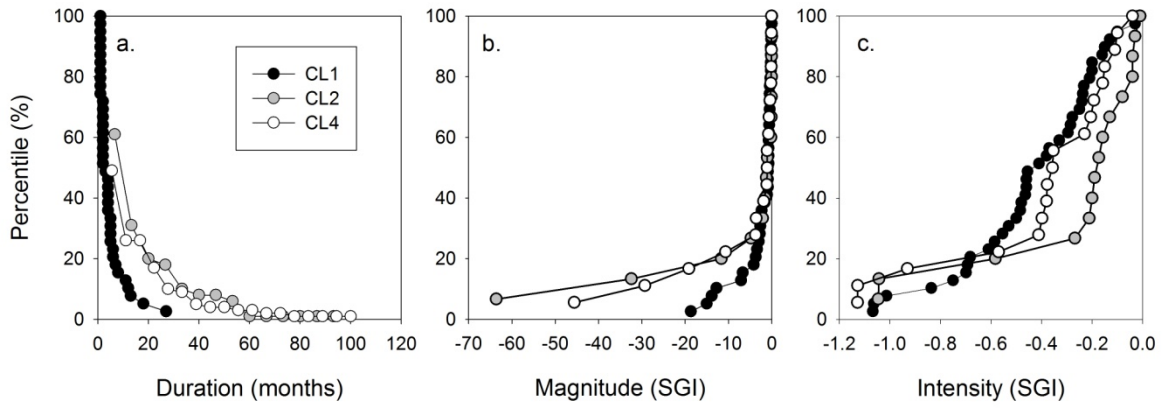
1037 Figure 10.



1038

1039

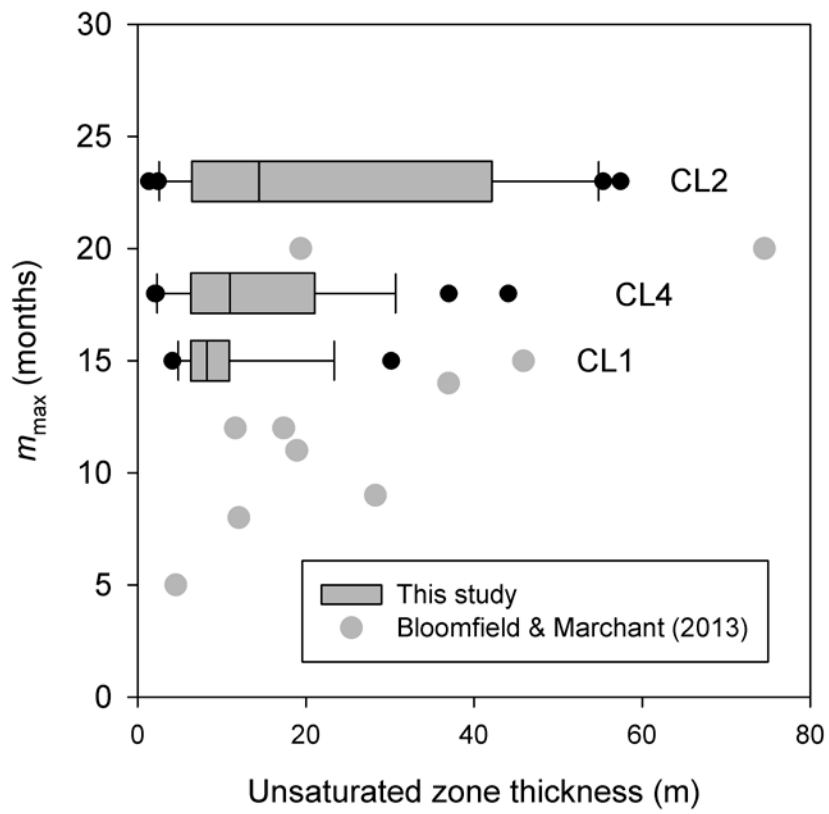
1040 Figure 11.



1041

1042

1043 Figure 12.



1044